



The marine $\delta^{18}\text{O}$ record overestimates continental ice volume during Marine Isotope Stage 3

April S. Dalton^{a,*}, Tamara Pico^b, Evan J. Gowan^{c,d,e}, John J. Clague^f, Steven L. Forman^g, Isabelle McMartin^h, Pertti Sarala^{i,j}, Karin F. Helmens^{k,l}

^a Department of Physical Geography and Geoecology, Charles University, Prague, Czech Republic

^b Caltech, Pasadena, CA, United States

^c Alfred Wegener Institute, Helmholtz Centre for Polar and Marine Research, Bremerhaven, Germany

^d MARUM, University of Bremen, Bremen, Germany

^e Department of Earth and Environmental Sciences, Kumamoto University, Kumamoto, Japan

^f Department of Earth Sciences, Simon Fraser University, Burnaby, British Columbia, Canada

^g Department of Geosciences, Baylor University, Waco, TX, United States

^h Geological Survey of Canada, Natural Resources Canada, Ottawa, Ontario, Canada

ⁱ Oulu Mining School, P.O. Box 3000, FI-90014, University of Oulu, Finland

^j Geological Survey of Finland, P.O. Box 77, FI-96101 Rovaniemi, Finland

^k Värriö Research Station, Institute for Atmospheric and Earth System Research INAR / Physics, P.O. Box 64, FI-00014, University of Helsinki, Finland

^l Swedish Museum of Natural History, P.O. Box 50007, 10405 Stockholm, Sweden

ARTICLE INFO

Editor: Dr. Alan Haywood

Keywords:

Mid-Wisconsinan

Mid-Weichselian

Global mean sea level

Fennoscandian

Laurentide

Cordilleran

ABSTRACT

There is disagreement in the Quaternary research community in how much of the marine $\delta^{18}\text{O}$ signal is driven by change in ice volume. Here, we examine this topic by bringing together empirical and modelling work for Marine Isotope Stage 3 (MIS 3; 57 ka to 29 ka), a time when the marine $\delta^{18}\text{O}$ record indicates moderate continental glaciation and a global mean sea level between -60 m and -90 m. We compile and interpret geological data dating to MIS 3 to constrain the extent of major Northern Hemisphere ice sheets (Eurasian, Laurentide, Cordilleran). Many key data, especially published in the past ~ 15 years, argue for an ice-free core of the formerly glaciated regions that is inconsistent with inferences from the marine $\delta^{18}\text{O}$ record. We compile results from prior studies of glacial isostatic adjustment to show the volume of ice inferred from the marine $\delta^{18}\text{O}$ record is unable to fit within the plausible footprint of Northern Hemisphere ice sheets during MIS 3. Instead, a global mean sea level between -30 m and -50 m is inferred from geological constraints and glacial isostatic modelling. Furthermore, limited North American ice volumes during MIS 3 are consistent with most sea-level bounds through that interval. We can find no concrete evidence of large-scale glaciation during MIS 3 that could account for the missing ~ 30 m of sea-level equivalent during that time, which suggests that changes in the marine $\delta^{18}\text{O}$ record are driven by other variables, including water temperature. This work urges caution regarding the reliance of the marine $\delta^{18}\text{O}$ record as a de facto indicator of continental ice when few geological constraints are available, which underpins many Quaternary studies.

1. Introduction

The Quaternary is characterized by continental ice volume changes in the Northern Hemisphere associated with 130 to 145 m of sea-level change (Fox-Kemper et al., 2021). The timing and distribution of these glaciations, except for the last glacial maximum (LGM) at 26.5–19 ka (Clark et al., 2009), are poorly understood owing to a highly fragmented

geological record and limited age control. To circumvent the lack of empirical constraints, the marine $\delta^{18}\text{O}$ record is predominantly used to estimate the volume of continental ice (upper plot; Fig. 1); a relative enrichment of ^{18}O in seawater is linked to significant ice accumulation on the continents (around 5‰ during the last glacial maximum at ~ 25 ka), whereas a decrease is associated with a turn toward non-glacial conditions (around 3‰ during the last interglacial at 125 ka; Adkins

* Corresponding author.

E-mail address: april.s.dalton@gmail.com (A.S. Dalton).

<https://doi.org/10.1016/j.gloplacha.2022.103814>

Received 29 April 2021; Received in revised form 5 April 2022; Accepted 8 April 2022

Available online 19 April 2022

0921-8181/© 2022 Elsevier B.V. All rights reserved.

et al., 2002; Berger et al., 2016; Elderfield et al., 2012; Lisiecki and Raymo, 2005; Schrag et al., 1996; Sosdian and Rosenthal, 2009). Other factors complicate the translation of marine $\delta^{18}\text{O}$ data to continental ice volume, notably variations in surface and deep-water temperatures that account for 0.4 to 1.0‰ of the difference between glacial and interglacial conditions (Adkins et al., 2002; Elderfield et al., 2012; Hastings et al., 1998; Lea et al., 2000; Schrag et al., 1996; Sosdian and Rosenthal, 2009; Tierney et al., 2020). Explaining the effects of ice volume, temperature, salinity and source/transport distance through the Quaternary remains a key challenge for Quaternary workers (Tierney et al., 2020). Nevertheless, recognizing the limitations of the marine $\delta^{18}\text{O}$ record, there appears to be broad agreement that at least half (possibly >70%) of the signal is driven by land ice (De Boer et al., 2014), and the marine $\delta^{18}\text{O}$ record has become a key indicator of continental ice volume (and a solution for concomitant sea-level expression) during intervals when few geological and age constraints are available (e.g. Batchelor et al., 2019).

Marine Isotope Stage 3 (MIS 3; 57 ka to 29 ka) offers a useful time period for comparing continental ice estimates derived from the marine $\delta^{18}\text{O}$ record to the empirically constrained footprint of Northern Hemisphere ice sheets and equivalent global mean sea level (GMSL). Importantly, MIS 3 aged geological deposits are more readily available and more easily datable than those of earlier intervals of the Quaternary. Marine Isotope Stage 3 was an interval where the marine $\delta^{18}\text{O}$ record indicates gradual continental ice growth toward the last glacial maximum (LGM; upper plot; Fig. 1). Accordingly, traditional paleogeographic reconstructions have portrayed moderate continental glaciation during that interval (e.g. Dredge and Thorleifson, 1987; Dyke et al., 2002). However, recent stratigraphic studies have reported new geochronological and biostratigraphic data from the core of glaciated regions that argue for significant changes in Northern Hemisphere ice extent during MIS 3 (Dalton et al., 2016; Helmens, 2014; McMartin et al., 2019; Sarala et al., 2016; Wohlfarth, 2010). Furthermore, recent

glacial isostatic adjustment modelling efforts support the feasibility of reduced ice cover and volume in some key areas of the formerly glaciated region (Gowan et al., 2021; Pico et al., 2018; Pico et al., 2017). Together, these data indicate substantial variability in the spatial distribution of MIS 3 continental ice that motivates a comparison to the marine $\delta^{18}\text{O}$ record.

Siddall et al. (2008) provided the most comprehensive overview of sea level data during MIS 3. They used several ^{18}O proxy records and coral-based sea level indicators to constrain variations in sea level. In that paper, proxy-based estimates were tuned on the basis of an assumed LGM sea level of -120 m and the results suggested four or five fluctuations in sea level during MIS 3, with a magnitude of 10–30 m. Siddall et al. (2008) also proposed that the first half of MIS 3 had an average sea level of about -60 m and the second half of about -80 m, though with uncertainties on these estimates on the order of ± 30 m.

Here, we examine how well the marine $\delta^{18}\text{O}$ record estimates continental ice volume during MIS 3 by reviewing recent empirical evidence, modelling outcomes and other global sea level records. First, existing estimates are summarized for past global mean sea level during MIS 3. Then, the geological data that constrain the footprint of MIS 3 ice sheets for key regions of the Northern Hemisphere (Eurasian, Laurentide, and Cordilleran) are discussed to ascertain the variability of the spatial extent of continental ice at that time. To infer continental ice volume, we summarize results from recent modelling studies of glacial isostatic adjustment, including estimated ice sheet thickness based on equilibrium ice sheet physics. We emphasize the variability of Northern Hemisphere ice extents, where it is believed the largest changes in ice volume occurred (Clark et al., 2009).

2. Global mean sea level during MIS 3

Direct physical evidence for sea-level changes prior to the LGM is difficult to obtain because records of GMSL have been largely obliterated

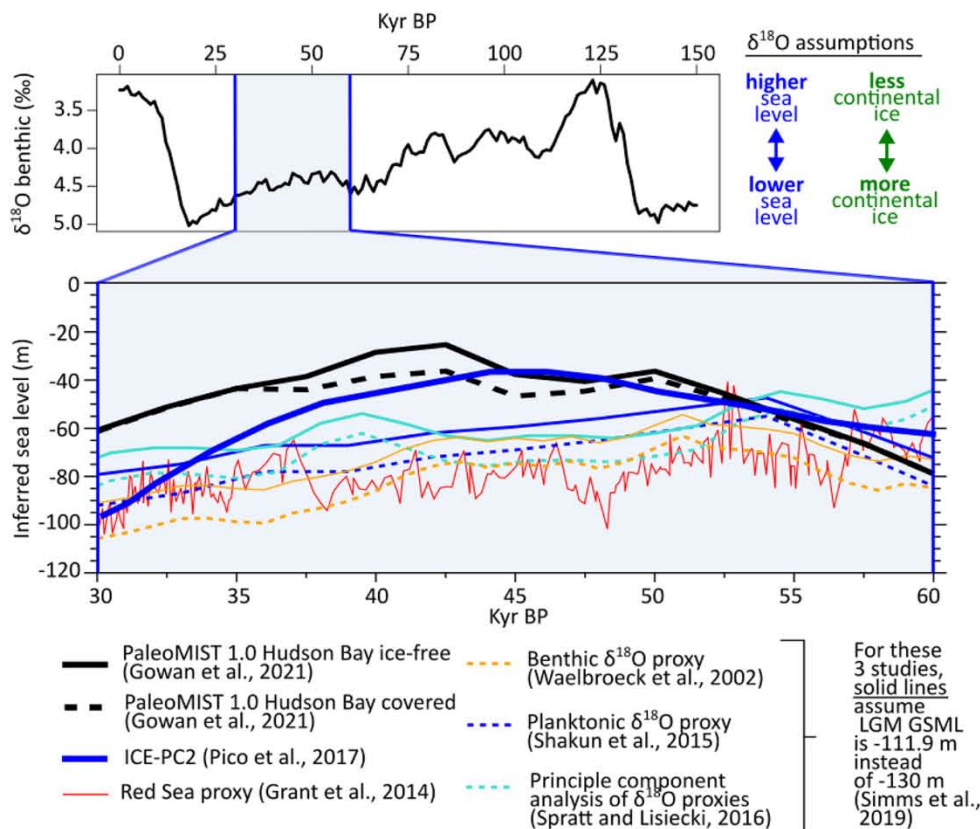


Fig. 1. Benthic $\delta^{18}\text{O}$ data through the last glacial cycle (upper plot; Lisiecki and Raymo, 2005) along with sea level during Marine Isotope Stage 3 (~57 ka to ~29 ka), inferred using various oxygen isotopic methods (lower plot). These records were corrected for temperature effects in the original studies. The dashed lines indicate a recalculated inferred sea level based on a LGM eustatic sea level of -111.9 m (Simms et al., 2019) rather than -130 m assumed in the original studies. Also included are three GMSL curves from the ice sheet reconstruction by Gowan et al. (2021), which are fitted within the empirically constrained footprint of Northern Hemisphere ice sheets, as well as ICE-PC2 (Pico et al., 2017). Note the significantly higher sea level calculated by Gowan et al. (2021) during MIS 3 than what was inferred from oxygen isotopic records.

by more recent events, such as ice advance and postglacial sea level rise. Accordingly, estimates of past GMSL are often instead inferred from various $\delta^{18}\text{O}$ proxy records, such as global oxygen isotopic records from benthic foraminifera (Waelbroeck et al., 2002; temperature signal removed via statistical method); planktonic foraminifer stacks (Shakun et al., 2015; temperature signal removed using a Mg/Ca proxy); restricted basins such as the Red Sea (Grant et al., 2014; temperature effect assumed to be small); and statistical analysis of multiple datasets (Spratt and Lisiecki, 2016; seven records all corrected for temperature effects). These records yield an inferred GMSL between -60 and -90 m for MIS 3, without accounting for uncertainties (lower plot; Fig. 1). A thorough review of the sea level records is beyond the scope of this paper. However, additional commentary on these records is provided in the Discussion.

3. Footprint of Northern Hemisphere ice during MIS 3

Geological sites dating to MIS 3 are widespread in the glaciated region of the Northern Hemisphere (Fig. 2). Many key geochronological data have been published over the past ~ 15 years with substantially improved techniques (e.g. targeted radiocarbon dating of terrestrial plants; and optically stimulated luminescence dating using single-aliquot regenerative-dose or single grains). Thus, there are presently many high-resolution geological records with multiple age constraints and/or chronological control combining different dating techniques that lend credibility to the MIS 3 age assignment. The Eurasian, Laurentide and Cordilleran are three major Northern Hemisphere ice masses.

3.1. Eurasian Ice Sheet

Early studies on the Late Quaternary glacial history of Fennoscandia (northern Europe) were hampered by a highly fragmented sedimentary

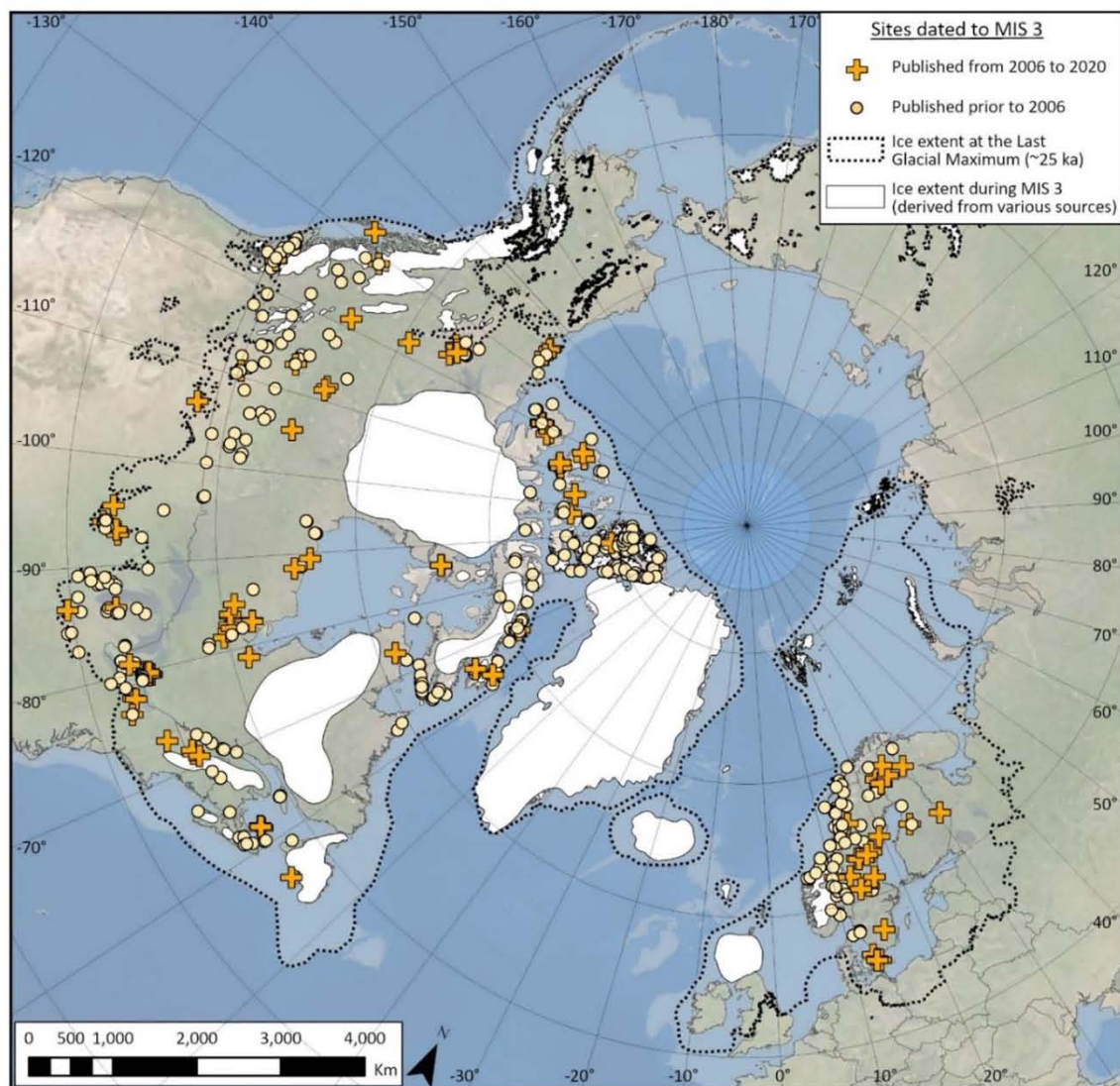


Fig. 2. Available geological sites in the Northern Hemisphere that date to Marine Isotope Stage 3 (~ 57 ka to ~ 29 ka), grouped by age of publication (<15 years old = orange cross; >15 years old = point). Also shown is the hypothesized extent of MIS 3 ice. The Cordilleran Ice Sheet is a new interpretation based on scrutiny of the geological dataset (see Fig. 6), the Laurentide and Scandinavian ice sheets are based on previous work (Arnold et al., 2002; Dredge and Thorleifson, 1987), and the extent of other ice masses (notably, those not undergoing significant change during MIS 3, for example Greenland) are based on a previous review (Batchelor et al., 2019). The last glacial maximum (~ 25 ka) is shown as a black dotted line, after Batchelor et al. (2019). The geological sites, located well-within the region glaciated at the last glacial maximum, support a significant reduction in Northern Hemisphere ice during MIS 3. Data from North America were compiled previously (Dalton et al., 2019; Dalton et al., 2022), and European data are from a variety of sources including Wohlfarth (2010), Ukkonen et al. (2007), Sarala et al. (2016) and Alexanderson et al. (2010). All MIS 3 publications are listed in Appendix A.

record and limited age control (Andersen and Mangerud, 1989; Donner, 1995; Hirvas, 1991; Lundqvist, 1992; Mangerud, 1991). At that time, reconstructions were tentative and largely in agreement with the record of global ice volume changes inferred from the marine $\delta^{18}\text{O}$ record. Based upon the latter, it was assumed that most parts of Fennoscandia were covered by an ice sheet during the entire MIS 4 interval (71 ka to 57 ka) to MIS 3.

More recently, large-scale ice-free conditions in Fennoscandia during

MIS 3 have been suggested based on extensive radiocarbon, optically stimulated luminescence and thermoluminescence datasets from Norway (Olsen et al., 2001a; Olsen et al., 2001b), Denmark (Houmark-Nielsen and Kjær, 2003), Finland (Helmens, 2014; Johansson et al., 2011; Mäkinen, 2005; Sarala, 2005; Sarala, 2019) and Sweden (Wohlfarth, 2010). Importantly, key sites have been revisited and new sites have been studied using improved dating techniques (e.g. accelerator mass spectrometry ^{14}C dating on carefully selected macrofossil remains

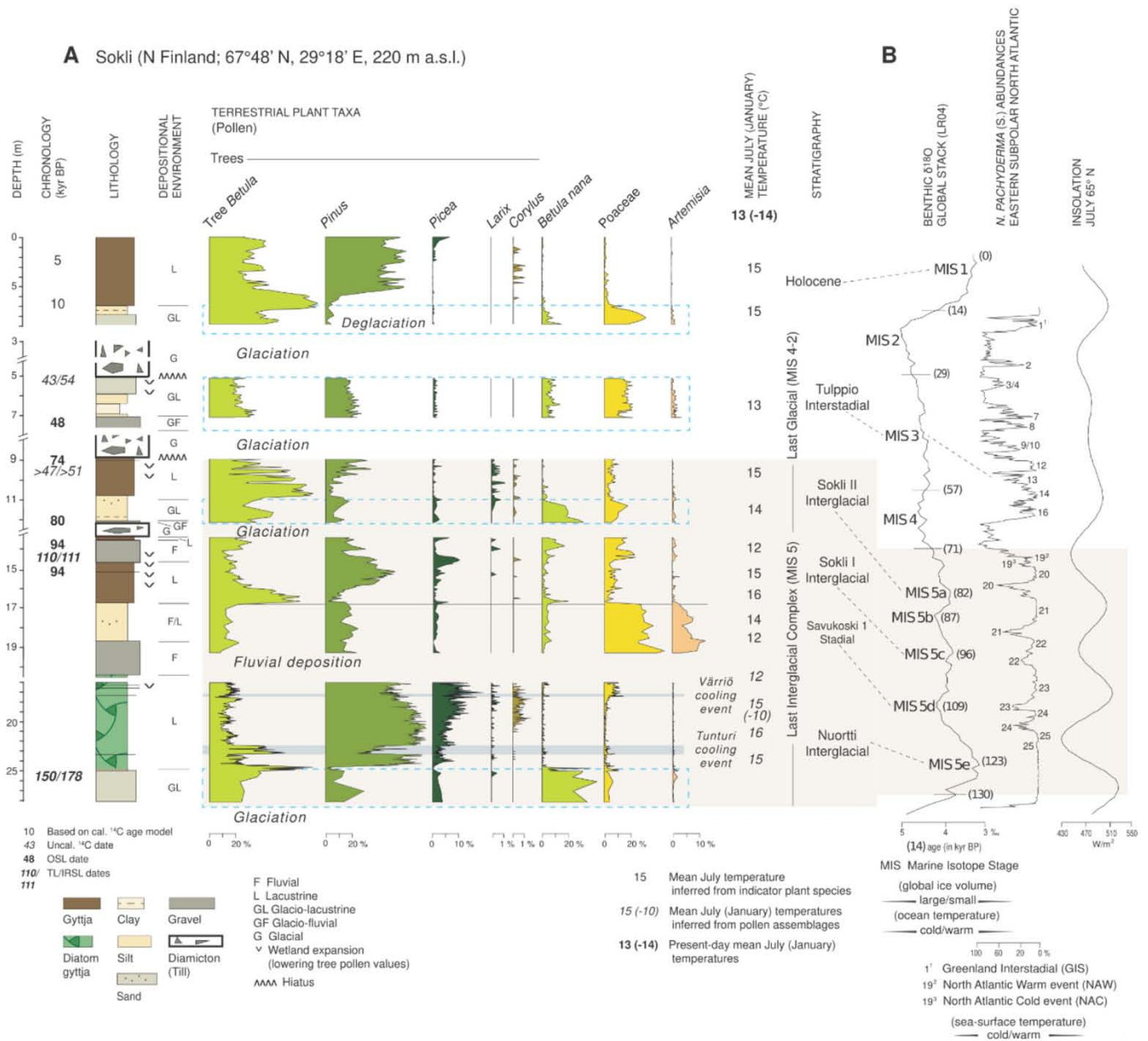


Fig. 3. A. A selection of late Quaternary environmental proxies and inferred temperature values for the Sokli site (NE Finland) situated in the central area of Fennoscandian glaciation. Warm interglacial conditions with developments toward boreal forest and summer temperatures exceeding present-day values are recorded for all three warm stages of MIS 5 (i.e. 5e, 5c, 5a) and the Holocene. The area was further ice-free during MIS 5d and early MIS 3 when steppe-tundra (MIS 5d) and low-arctic shrub tundra vegetation types (MIS 3) developed. Note that the lake deposit of early MIS 3 age, as well as of MIS 5a age, are truncated and only record the early part of these warm stages. At the nearby Kaareoja site, the development toward birch forest with local stands of pine trees is reported for early MIS 3 (Sarala et al., 2016). The early MIS 3 and MIS 5e, 5c and 5a warm stages coincide with periods of higher-than-present insolation at high northern latitudes (see B in figure). B. Late Quaternary stratigraphies in marine sediments, globally according to Lisiecki and Raymo (2005) and for the eastern subpolar North Atlantic following McManus et al. (1994) and Bond et al. (1993); Greenland Interstadials are after Johnsen et al. (1992) and Dansgaard et al. (1993). The benthic $\delta^{18}\text{O}$ stack is a proxy for global ice volume and ocean temperature and the record of *N. pachyderma* (s.) abundances for sea-surface temperature. Variations in summer insolation at high northern latitudes (Berger and Loutre, 1991) are indicated to the right. Adapted from Helmens (2014) with new data from Sokli as presented in Salonen et al. (2018) and Helmens et al. (2021); Helmens et al. (2018).

of terrestrial plants) that support earlier published datasets and interpretations (Alexanderson et al., 2010; Howett et al., 2015; Kleman et al., 2020; Lunkka et al., 2008; Lunkka et al., 2015; Möller et al., 2020; Möller et al., 2013; Paus et al., 2011; Salonen et al., 2008; Salonen et al., 2014; Sarala and Eskola, 2011). Notably, a key Late Quaternary sedimentary sequence preserved at Sokli, northern Finland, indicates ice-free conditions in what is the near-central area of Fennoscandian glaciation at least during part of early MIS 3 (Fig. 3; Helmens et al., 2007; Helmens et al., 2009). The same features are also seen in Kaareoja, northernmost Finland, where a full interstadial sediment succession with associated vegetation record is inferred during MIS 3 (Sarala et al., 2016). An objective margin reconstruction of the mid-MIS 3 period (34 ka to 38 ka) based on many of these data, depicts ice cover being restricted to mountainous regions of Norway and Sweden (Hughes et al., 2016).

The MIS 3 interstadial vegetation in Fennoscandia was mostly open and pioneer birch-dominated (Helmen, 2014). Rapidly responding aquatic taxa (plants, insects) record high insolation-forced, warm summers (Bos et al., 2009; Engels et al., 2008; Helmens et al., 2007; Sarala et al., 2016; Väliaranta et al., 2012). To the west, in the Norwegian Sea, enhanced accumulation rates of ice-rafted debris between 50 ka and 35 ka compared with the Holocene (Baumann et al., 1995) indicates the existence of local, mountain-centered ice caps. The reconstructed dry continental climate for stadials on land (Alexanderson et al., 2011; Hättestrand and Robertson, 2010; Helmen, 2014) and their relatively short duration, however, suggests a spatially restricted ice cover (compared to the LGM) over Fennoscandia between ~50 and ~35 ka. To the southwest of Fennoscandia, the last Celtic Ice Sheet only expanded over Scotland after ~35 ka (Ballantyne and Small, 2019), and, to the northeast, the Barents and Kara Seas were probably ice-free between ~45 and ~20 ka (Larsen et al., 2006). Collectively, the data show ice-free conditions persisted over large parts of northern Europe, possibly interrupted by glaciation, in the time interval between ~50 and

~35 ka.

3.2. Laurentide Ice Sheet

Knowledge of North American glaciation has evolved considerably over time, starting with a hypothesis of several independent glaciers in the late 1800s (Tyrrell, 1898), then moving toward a model with a large-domed Laurentide Ice Sheet at the LGM (Flint, 1943). Extensive stratigraphic records dating to MIS 3 are found throughout the glaciated region of North America (notably, the St. Lawrence Lowlands, Southern Quebec Appalachians, Maritimes, Southern Ontario). However, the stratigraphic record in the Hudson Bay Lowlands (non-glacial deposits consisting of inter-till wood, peat, shells, and fluvial sediments) offers critical evidence on former ice dynamics for North America owing to its position at the geographic center of the Laurentide Ice Sheet. Based on an analysis of available geochronology data from this region in the 1980s (Andrews et al., 1983; Berger and Nielsen, 1990; Forman et al., 1987), Dredge and Thorleifson (1987) hypothesized both a large and small ice extent over North America during MIS 3. The reduced ice model, based largely on radiocarbon ages from shells, was met with criticism that cited the likelihood of modern-carbon contamination. Accordingly, the large ice model (showing ice covering Hudson Bay) prevailed as the more likely scenario (Thorleifson et al., 1992) and was adopted into subsequent ice sheet literature (notably, Dyke et al., 2002).

More recently, radiocarbon and luminescence dating of the stratigraphic record preserved in the Hudson Bay Lowlands suggests the geographic center of the Laurentide Ice Sheet was ice-free during some interval (s) of MIS 3 (Dalton et al., 2016). These data include numerous stratigraphic sections, found largely along riverbanks, bearing inter-till wood, peat, shells, and fluvial sediments that have been dated using several methods (Fig. 4). At sites where material was available, multiple dating attempts were made. Pollen data for the ice-free interval suggest a climate slightly cooler and drier than present day (Dalton et al., 2017).

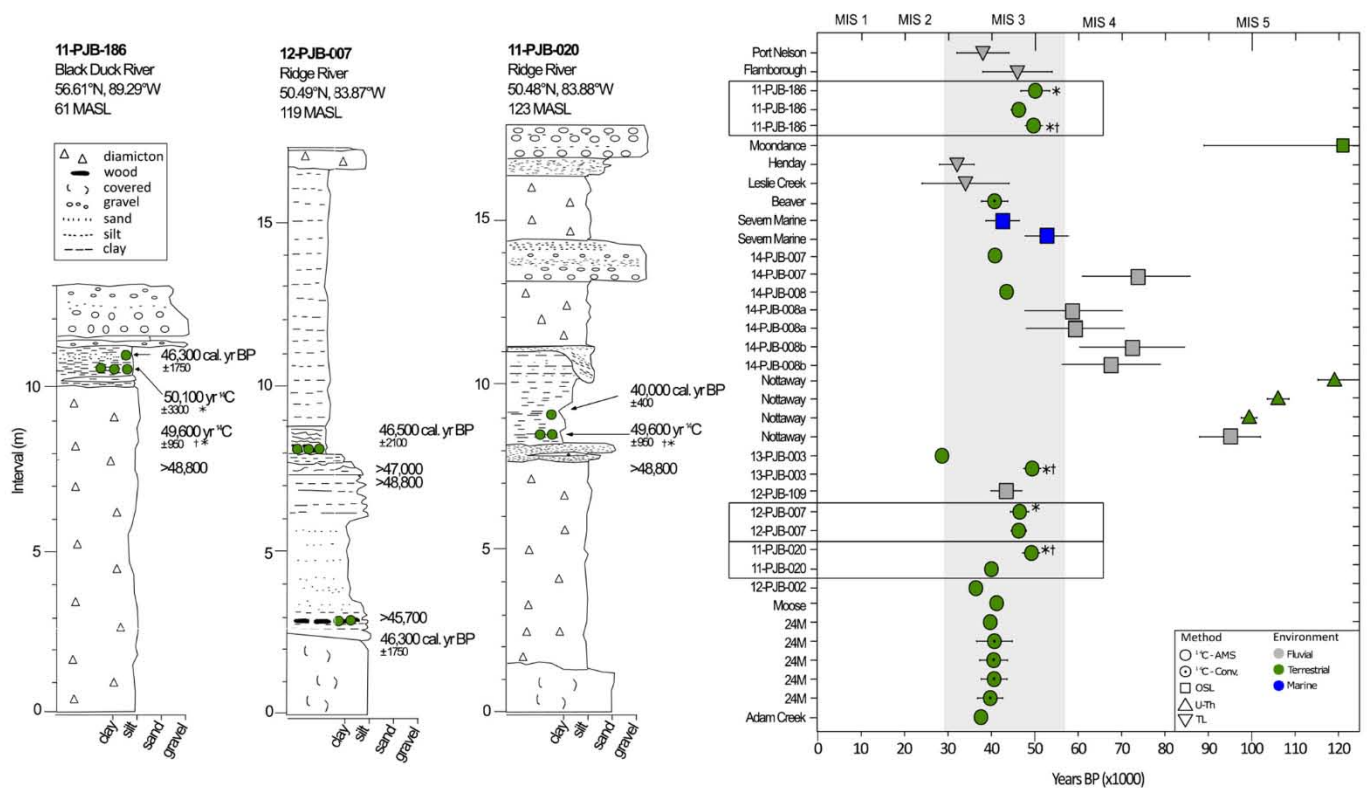


Fig. 4. Key stratigraphic and chronological data from the Hudson Bay Lowlands, Canada. These data suggest an ice-free geographic center of the Laurentide Ice Sheet during MIS 3. Figure modified from Dalton et al. (2016); bar plot includes additional optically stimulated luminescence ages from Dalton et al. (2018).

There is no direct evidence of an ice margin nearby. However, the interstadial climate suggests ice lobes may have persisted in Labrador and Keewatin, thus we adopt the mid-Wisconsinan minimal ice limits (Hypothesis 2) first proposed, but not favored, by Dredge and Thorleifson (1987). Although the duration of the hypothesized retreat is unknown, glacial isostatic adjustment studies based on fitting sea-level records along the east coast of the United States require minimal ice sheet loading in eastern Canada from 80 ka through mid-MIS 3 (Pico et al., 2017).

Additional evidence for ice-free conditions near the geographic center of the Laurentide Ice Sheet comes from radiocarbon dating of glacially transported marine mollusks in northwest Hudson Bay near Repulse Bay (Rae Isthmus ice stream; McMartin et al., 2019). In that area, eight shell samples from five sites yielded finite radiocarbon ages ranging from 35.8 ± 0.5 ka to 42.4 ± 0.5 ka (calibrated using Calib 8.1.0 and Marine 20 with 1σ error; Heaton et al., 2020; Reimer et al., 2020; Stuiver and Reimer, 1993). Field duplicates were collected at one site and aliquots at two sites were analyzed in separate laboratories. Physical pretreatment of the shells prior to etching included removal of the outer chalky layer or any visible contamination including encrustations of secondary carbonates or lichen. The cleaned fragments were then dissolved in dilute acid to further remove a portion of the shells' exterior, and calcite components with different percentages were removed depending on the sample cleanliness and size (10–50% removal) before AMS analysis. One of the possible pathways for a MIS 3 marine incursion

in this area is through the development of a calving bay from the east up Hudson Strait (McMartin et al., 2019). Shell ages in the >30 ka range are contentious owing to the possibility of modern carbon contamination during burial or surface weathering (e.g. Douka et al., 2010b; Miller and Andrews, 2019). Although such contamination by small amounts ($<1\%$) of young carbon cannot be entirely discounted, rigorous physical and chemical pretreatment of the samples increases the chance of measuring indigenous ^{14}C from the remaining hard, primary core of aragonite and minimizes the effects of secondary carbonate components. To more accurately evaluate the potential effects of recrystallization during burial, the identification of diagenesis could be achieved through the determination of mineralogical phases using high-precision methods (ie. Douka et al., 2010a; Douka et al., 2010b). In addition, independent dating techniques can be used to validate the radiocarbon chronology (see McMartin et al., 2019). The location of the MIS 3 shells in streamlined calcareous till on a plateau above the local (Holocene) marine limit (Fig. 5) coincides with a relatively old terrain that has largely escaped the deglacial ice flows into Repulse Bay (McMartin et al., 2021), whereas the Holocene shells collected in the same setting but below the marine limit are compatible with regional radiocarbon ages indicating a minimum deglaciation age of 8 ka. This grouping, together with the careful pretreatments used here, suggest relatively minor post-depositional alterations to the ages and support a marine episode prior to LGM in northwestern Hudson Bay. Contamination by old carbon in ocean waters or carbonate substrates is also a possibility, but this would

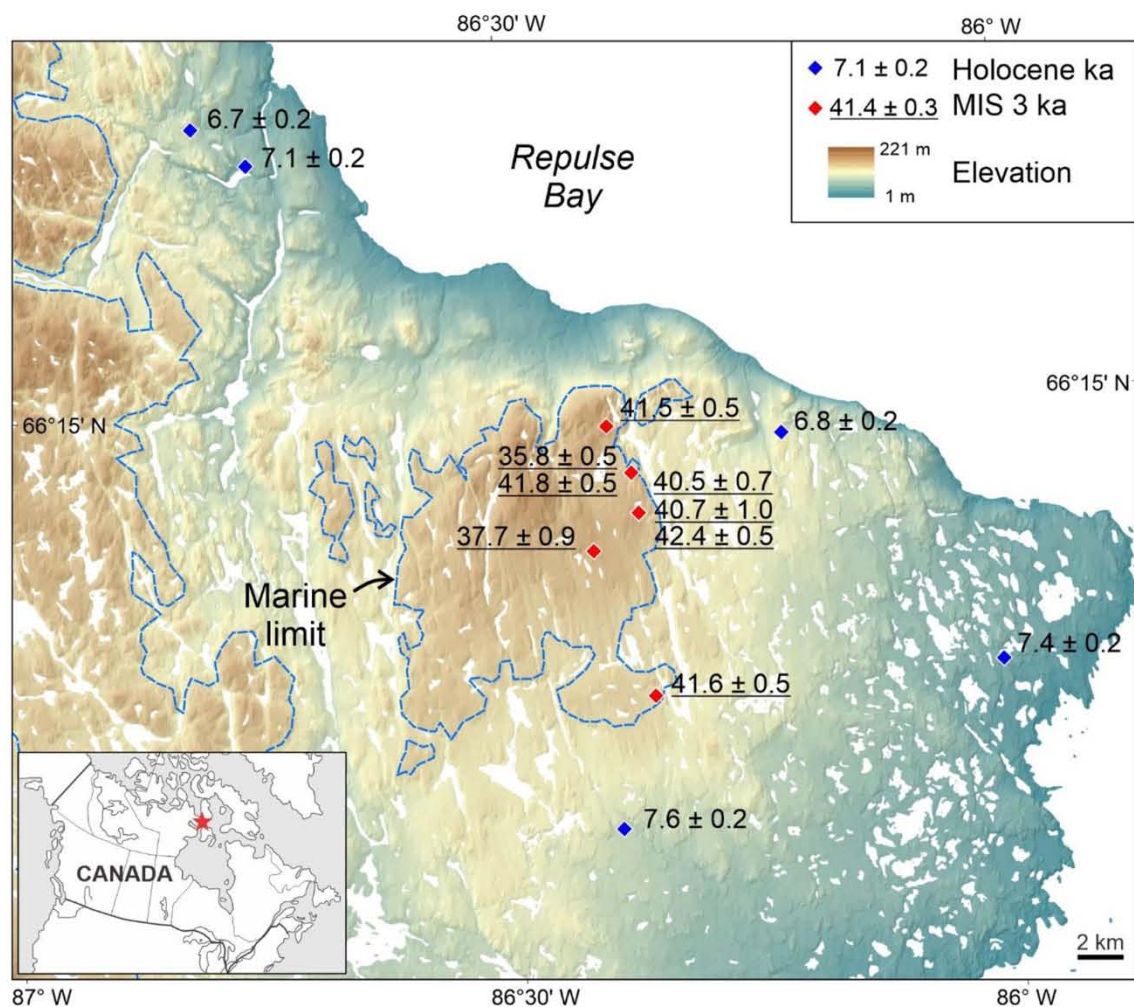


Fig. 5. Calibrated marine shell samples dating to MIS 3 collected in Rae Isthmus ice stream till south of Repulse Bay, Canada (modified from McMartin et al., 2019). All ages are given in thousand years BP and calibrated using Calib 8.20 and the Marine 20 curve (Heaton et al., 2020; Reimer et al., 2020; Stuiver et al., 2021). ($\Delta R = 152 \pm 37$ years; ages reported within 2σ error).

only make ages a few hundred to a few thousand years too old (Bezerra et al., 2000), and the ages of the Repulse Bay shells would remain within the MIS 3 period.

3.3. Cordilleran ice sheet

The Olympia Interglaciation, first defined by Armstrong et al. (1965), was an interval prior to the LGM when ice was absent from much of the Cordillera in western North America. Locally, the Olympia Interglaciation is recorded by the Bessette Sediments (Fulton, 1968; Fulton and Smith, 1978) and the Cowichan Head Formation (Alley, 1979; Armstrong and Clague, 1977), with finite radiocarbon ages from beyond the radiocarbon dating limit (>45 ka) to 20 ka (Clague, 1981; Hebda et al., 2016; Hickin et al., 2016; Mathewes et al., 2019). These MIS 3 sediments are present in coastal lowlands and interior valleys within the limit of the LGM Cordilleran Ice Sheet and comprise a wide variety of non-glacial sediments, some with forest beds and, locally, the remains of fossil bison, horse, and mammoths.

We present a novel hypothesis of Cordilleran ice extent during MIS 3 (Fig. 6) where ice is restricted to montane source areas. The absence of ice in intermontane areas and coastal lowlands is suggested by our compilation of >90 radiocarbon ages from the Bessette sediments and Cowichan Head Formation, correlative strata, and from Late

Wisconsinan advance outwash (Quadra Sand). Our hypothesis indicates that lowland areas, interior valleys, and intermontane plateaus in at least southern and central British Columbia were ice-free continuously for several tens of thousands of years during MIS 3. This interpretation is supported by paleoecological work on the Olympia nonglacial deposits which suggests a climate during MIS 3 that was similar to or cooler than today (fossil beetles and pollen analysis; Alley, 1979; Armstrong and Clague, 1977; Clague et al., 1990; Harington et al., 1974), therefore regional conditions were likely insufficiently cold and wet to allow glacier advance beyond montane source areas into intermontane areas and coastal lowlands. Our empirically based ice depiction is in broad agreement with model simulations that suggest reduced Cordilleran ice cover during MIS 3 (Seguinot et al., 2016). Dynamic Cordilleran ice during MIS 3 is also supported by increased ice-rafted debris into the Pacific Ocean at that time (Walczak et al., 2020). Although MIS 3 Cordilleran ice cover was certainly much greater than today, the totality of evidence indicates that ice cover was much less than at the LGM.

4. Ice sheet volumes in the Northern Hemisphere from numerical modelling

Direct constraints on GMSL and ice thickness during MIS 3 are limited because of poor preservation in the paleorecord. Nevertheless, to evaluate the discrepancy between the estimates of GMSL derived from the marine $\delta^{18}\text{O}$ record and the empirically constrained footprint of Northern Hemisphere ice, we compare prior studies aimed at constraining ice sheet volumes during MIS 3 to the ice volume inferred from the marine $\delta^{18}\text{O}$ record (-60 to -90 m sea level equivalent; Fig. 1). Recent glacial isostatic adjustment studies suggest peak global mean sea level reached 30 to 50 m during mid-MIS 3. An analysis of sea-level markers in sediment cores in the Bohai Sea, which accounted for glacial isostatic adjustment, sediment compaction, and sediment loading, found that peak global mean sea level reached approximately -40 m (Pico et al., 2016). A later study used anomalously high sea-level records along the east coast of the United States to infer that the eastern Laurentide Ice Sheet grew rapidly from mid-MIS 3 leading to the LGM, suggesting North American ice sheets were the major contributor to a rapid global sea level fall from MIS 3 to the LGM (Pico et al., 2017). Furthermore, glacial isostatic adjustment simulations involving a late and rapid growth of the Laurentide Ice Sheet were shown to be consistent with most sea-level bounds associated with non-glacial deposits of MIS 3 age in Canada (Fig. 8; Pico et al., 2018).

Recently, Gowan et al. (2021) revisited these studies using glacial isostatic adjustment simulations with ice sheet history reconstructions determined using a simplified ice model constrained by geologic evidence of ice margin positions, sea level, and ice flow direction. Based on limited ice volume increases relative to present in most ice sheets (see sections above), this study assumed the main source of global ice volume change was due to variations in the Laurentide Ice Sheet. Fig. 7 shows the two hypothesized ice sheet configurations presented in this study: one with an ice free Hudson Bay (e.g. Dalton et al., 2019), and one where Hudson Bay remains ice covered (e.g. Miller and Andrews, 2019). The configuration was adjusted to ensure the surface slope of the ice sheet was in the direction of known ice flow direction indicators (e.g. Gauthier et al., 2019). Fluctuations in the ice sheet extent were assumed to coincide with the timing of Heinrich Events (Andrews and Voelker, 2018), which may have caused fluctuations in eustatic sea level on the order of 5 to 10 m (Chappell, 2002; Yokoyama et al., 2001). The study found that sea-level simulations using these ice sheet reconstructions fit the sea-level constraints in the Bohai Sea used in Pico et al. (2016) but not the east coast of the United States (Pico et al., 2017). This misfit is likely due to greater ice sheet loading in eastern Canada for the Gowan et al. (2021) reconstruction, whereas the Pico et al. (2017) study requires minimal ice loading in eastern Canada from 80 ka to 44 ka. Regardless of scenario, global mean sea level is calculated to remain above -50 m between 55 and 35 ka (see Fig. 1), in agreement with prior

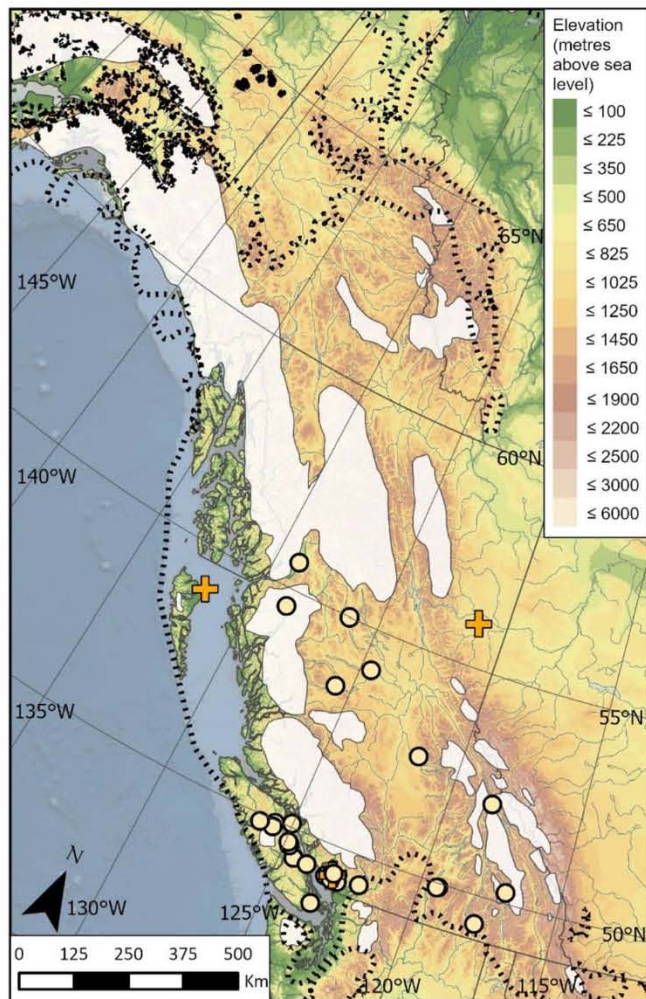


Fig. 6. Available geological sites in the footprint of the Cordilleran Ice Sheet that date to MIS 3, grouped by age of publication (<15 years old = orange cross; >15 years old = point). The presence of MIS 3 sediments in coastal lowlands and interior valleys suggests a reduced Cordilleran Ice Sheet at that time. A listing of all MIS 3 publications is available in Appendix A.

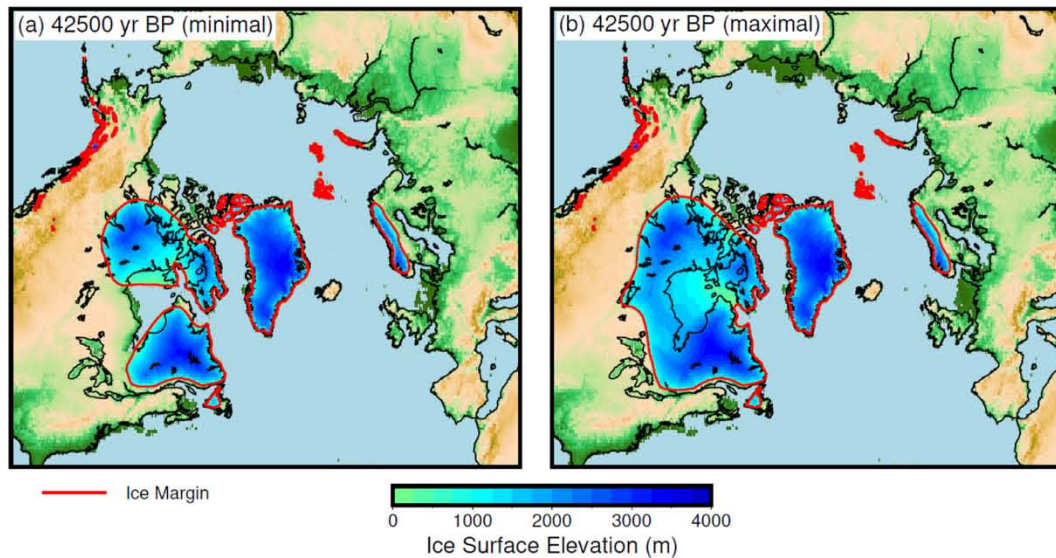


Fig. 7. Topography of Northern Hemisphere ice sheets during MIS 3 (42.5 ka) after Gowan et al. (2021). The minimal ice configuration (19 m SLE) shows a deglaciated Hudson Bay (as suggested by Dalton et al., 2019), whereas the maximal ice configuration (30 m SLE) shows this region fully glaciated (as suggested by Miller and Andrews, 2019). Both scenarios require sea level to be above -50 m between 55 and 35 ka, which is substantially higher than what has been inferred from oxygen isotopic records (see Fig. 1).

studies that inferred a global mean sea level peak of -38 ± 7 m (Pico et al., 2017; Pico et al., 2016). We stress that ice sheet reconstructions discussed here (Gowan et al., 2021; Pico et al., 2017) assume different ice configurations, in particular whether ice is present or absent over eastern Canada during MIS 3. Regardless, a common conclusion drawn by these studies is a higher GMSL during MIS 3 than predicted via the marine $\delta^{18}\text{O}$ record (Fig. 1). This global mean sea level inference suggests the volume of ice inferred from the marine $\delta^{18}\text{O}$ record is inconsistent with the empirically constrained footprint of Northern Hemisphere ice sheets during MIS 3.

Finally, we adopt a third approach to calculate ice volume and sea level changes during MIS 3. We import hypothesized Northern Hemisphere ice configurations by Batchelor et al. (2019), which are constrained by empirical data, where available, into the same setup used to create the PaleoMIST reconstructions (Gowan et al., 2021). Sea level equivalent is calculated by how much the ice volume in the ice sheets would uniformly lower sea level, based on modern day ocean area. In these tests, the maximum MIS 3 scenario from Batchelor et al. (2019) produces the largest volume of ice, with a sea level equivalent of 54 m (Table 1). The minimum scenario is 10 m, while the two PaleoMIST scenarios fall between these values. Because ocean area would shrink as the ice sheets grow, the actual sea level drop will be a few meters lower than what is presented in the table. Nevertheless, even in the maximum case at 45 ka, it is unlikely that ice sheets held more than 60 m of sea

level equivalent, which offers additional support for the hypothesis of actual relative sea level was higher than inferred from the $\delta^{18}\text{O}$ record during MIS 3.

5. Discussion

Our work suggests a discrepancy between the volume of continental ice inferred from the marine $\delta^{18}\text{O}$ record during MIS 3 (between -60 and -90 m of sea-level equivalent) and the volume of ice constrained using geological data (between -30 m and -50 m of sea-level equivalent). Some discrepancy may be expected given all uncertainties involved in translating marine $\delta^{18}\text{O}$ data to continental ice volume (e.g. uncertainties in past ocean temperature and salinity, as well as the distribution of continental ice sheets). We acknowledge the possibility of issues with the geochronological datasets (noted by the critiques of these datasets by Arnold et al., 2002; and Miller and Andrews, 2019). However, the magnitude of the discrepancy and the ensemble of empirical evidence supported by numerical models cannot be ignored.

5.1. Uncertainties in North American ice sheet extent during MIS 3

Readers should be aware of two differing hypotheses for North American ice sheet configuration during MIS 3. Fundamentally, both result in a higher GMSL during MIS 3 than predicted via the marine $\delta^{18}\text{O}$ record (see Fig. 1, Table 1, and Gowan et al., 2021). However, because they differ substantially in their depiction of ice coverage over North America, we consider a brief overview to be appropriate here. As outlined above (Section 3.2), radiocarbon and luminescence dating of the stratigraphic record preserved in and around Hudson Bay suggests the geographic center of the Laurentide Ice Sheet might have been ice-free during some interval (s) of MIS 3 (Dalton et al., 2016). However, Miller and Andrews (2019) argue that finite radiocarbon ages from the Hudson Bay Lowlands principally reflect contamination by contemporary carbon sources and that the geochronological argument for an ice-free Hudson Bay Lowlands during MIS 3 is flawed. Miller and Andrews (2019) also argue that thick ice over Hudson Bay is required for Heinrich Events. Dalton et al. (2016) scrutinized geochronological data from the Hudson Bay Lowlands and removed numerous radiocarbon ages from further consideration based on that possibility. However, Dalton et al. (2016) concluded that >35 ages (including radiocarbon dates on wood

Table 1

Calculation of sea level equivalent ice volume of Northern Hemisphere ice sheets during MIS 3.

Time	Batchelor et al. (2019) min	Batchelor et al. (2019) best	Batchelor et al. (2019) max	Gowan et al. (2021) PaleoMIST min	Gowan et al. (2021) PaleoMIST max
30 ka	39.1	48.1	82.3	44.6	45.1
35 ka	34.4	40.7	79.8	32.7	32.8
40 ka	14.6	19.3	79.0	21.6	31.7
45 ka	9.9	14.6	54.0	31.1	40.0

and optically stimulated luminescence ages) remain in support of local ice-free conditions during MIS 3. Subsequent scrutiny of the geochronological dataset by Miller and Andrews (2019) suggested that only two of the MIS 3 radiocarbon ages can ‘plausibly considered to be finite’.

Clearly, future chronostratigraphic work in the Hudson Bay Lowlands is critical for resolving the extent of North American ice sheets during MIS 3. Regarding radiocarbon dating, contamination by small amounts (<1%) of young carbon can make infinite ages to appear finite, particularly near the upper limit of the method (~50 to 35 ka; Taylor, 1987). It is therefore important to supplement radiocarbon chronologies with ages acquired using other techniques, when possible. Moreover, future work on these sediments should involve duplicates and replicates age samples, as well as exploration of filtered datasets, Bayesian modelling and appropriate pre-treatment methods (e.g. Douka et al., 2010b; Young et al., 2021). It is noteworthy that, outside of glaciated regions, late MIS 3 radiocarbon dates (ca. 30 to 45 ka) are routinely accepted and provide a chronological framework for late MIS 3 vegetation and climate dynamics that is in general agreement with the Greenland ice core and North Atlantic marine records (Behre and van der Plicht, 1992; Herring and Gavin, 2015; Nishizawa et al., 2013; Woillard and Mook, 1982). In this work, no large-scale rejections of MIS 3 radiocarbon ages have taken place.

Geochronological issues aside, removal of ice over the eastern sector of the Laurentide Ice Sheet leads to a significantly improved match with dated MIS 3 shorelines along the eastern United States (GIA work of Pico et al., 2017). Moreover, the stratigraphy of the Hudson Bay Lowlands directs to a severe reduction in ice extent at some point during the last glacial cycle. Notably, in the James Bay lowlands, thick sequences of varves occur between well-dated interglacial sediments (Allard et al., 2012) and LGM glacial deposits (Dubé-Loubert et al., 2013; Skinner, 1973), thus implying ice retreat beyond the James Bay region sometime between the last interglaciation (~125 to ~80 ka) and the LGM. Finally, from outside glaciated regions, high-resolution records of NH_4^+ soil emissions and wildfire activity in North America resolved from Greenland ice cores suggest long multi-millennial scale periods between 60 ka and 45 ka and again between 38 ka and 35 ka with peak soil NH_4^+ emissions and wildfire activity to near interglacial levels (Fischer et al., 2015). These proxy data suggest North America may not have sustained LGM-like ice cover through MIS 3. Alternatively, there may have been numerous intervals of ice sheet formation from plateau nucleation areas surrounding Hudson Bay and the subsequent collapse on multi-millennial time scales.

5.2. Searching for evidence of large Laurentide Ice Sheet during MIS 3

A large Laurentide Ice Sheet could account for the missing ~30 m of sea-level equivalent during MIS 3; thus, it is worth investigating all evidence related to the potential expansion of this ice mass. One of the few lines of evidence for a physical limit during MIS 3 is a moraine remnant in central Wisconsin, just beyond the LGM limit, that yielded a range of ^{10}Be surface exposure ages from 82 ka to 24.3 ka ($n = 16$). After removal of three outliers, the apparent age of this moraine is 35.8 ± 2.0 ka (Ceperley et al., 2019). The emplacement of this moraine might relate to a rapid advance from the Labrador Dome around 38 ka that has been associated with Heinrich Event 4 (Hemming, 2004). In this scenario, ice might have advanced over Lake Michigan (between 39.1 and 30.4 ka; Carlson et al., 2018) and potentially to almost LGM-extent in some areas south of the Great Lakes (optically stimulated luminescence dating and ^{14}C dating of proglacial lake sediments; Wood et al., 2010). However, this advance would have occurred after the minimal North American ice extent, and thus would not conflict with our hypothesis. Moreover, this cosmogenic age remains uncertain without a second radionuclide to correct ages for uncertainties related to surface weathering, moss and lichen growth, spallation and other processes (Ceperley et al., 2019).

Another piece of direct evidence for MIS 3 ice advance comes from tills in Iowa. Kerr et al. (2021) present radiocarbon ages from wood

bracketing tills that suggest short-lived ice advances from 45 ka to 35 ka (Fort Dodge advance) and from 34 ka to 30 ka (Lehigh advance). These data suggest a dramatic extension (ice stream?) of the Keewatin Dome southward through Manitoba at that time (Kerr et al., 2021). However, most of the Southern Plains remained ice-free (Bélanger et al., 2014; Burns, 1996). An early (MIS 3?) southeastward ice flow direction is recorded in eastern Manitoba, which supports a Keewatin-sourced ice advance (Gauthier and Hodder, 2020; Gauthier et al., 2019). The timing of the advances of this ice lobe may be reflected in a nearby speleothem record suggesting a relatively warm temperature early in MIS 3, with decided cooling post-55 ka (Dorale et al., 1998). Additional sediment provenance work suggests a potentially persistent extension of the Labrador Dome to almost LGM extent during parts of MIS 3 (Dendy et al., 2021). The precise configuration of these ice lobes (along with their total ice volume) is unclear. However, these data are suggestive of greater (or highly dynamic) ice cover over North America during MIS 3.

Over North America, there is some indirect proxy evidence suggesting a moderately large continental ice sheet during MIS 3. However, this evidence can be explained by non-glacial processes and/or the brief ice extension noted by Kerr et al. (2021). Notably, the eolian-sourced Roxana Silt (and correlatives, e.g. Gilman Canyon Formation) is spatially ubiquitous in the mid-continental United States and was deposited from 55 ka to 30 ka (Bettis et al., 2003; Follmer, 1996; Forman and Pierson, 2002; Leigh, 1994). This loess deposit was sourced from major river valleys and is associated with valley aggradation as an ice sheet advanced, similar to what was observed when LGM ice advanced into the region (Peoria Loess; Bettis et al., 2003). A salient observation is that large-scale valley aggradation and associated increases in sediment supply and eolian flux at the LGM and during MIS 3 have also occurred in drainages in southeastern and south-central North America, far removed from the direct effects of meltwater from the Laurentide Ice Sheet (Ivester et al., 2001; Leigh et al., 2004). These studies and others indicate that increased riverine sediment supply and net aggradation can reflect broader changes in seasonal precipitation, ecosystems and surface processes as climate oscillated in the late Quaternary, rather than solely indicate glaciation in a catchment.

Oxygen isotopic excursions that may be proxies for a large Laurentide Ice Sheet that breached the Mississippi River catchment have been inferred from sedimentary records from the Gulf of Mexico (Aharon, 2003; Flower et al., 2011; Sionneau et al., 2013; Tripanas et al., 2007). However, the meaning of negative oxygen isotopic excursions in MIS 3 remains unresolved. Significant negative isotopic excursions (>0.5‰) have been documented in cores from Bryant Canyon, Gulf of Mexico, at 37 ka, 45 ka and 53 ka, which were interpreted as brief episodes of meltwater flux with limited excursions of the Laurentide Ice Sheet into the Mississippi River drainage (Tripanas et al., 2007). In contrast, a subsequent analysis of these meltwater events in the Gulf of Mexico with added analysis of associated clay mineralogy indicates a non-glacial source for these isotopic excursions with enhanced contributions from western and northeastern sources (Sionneau et al., 2013). If these excursions were glacial in origin, they can be explained by the short dramatic extension (ice stream?) of the Keewatin Dome southward through Manitoba at that time (Kerr et al., 2021), which would account for only a very small ice volume given their presumably thin, streamlined natures and short-lived duration (Margold et al., 2015).

5.3. Searching for other stores of continental ice during MIS 3

The assumed main source of ice volume variations through the last glacial cycle was the Laurentide Ice Sheet (Clark et al., 2009; Stokes et al., 2012). However, the lack of support for a large Laurentide Ice Sheet during MIS 3 (see Section 5.2) may point toward the importance of other ice masses for hosting the missing ~30 m of sea-level equivalent. In Europe, some ice growth in northern Fennoscandia and northwestern Russia was possible during early MIS 3 (Svendsen et al., 2004). Mangerud et al. (2010) also provide evidence for ice expansion in Northern

Europe around 40 ka, but this likely had a local source (coastal Norwegian mountains) and provides no evidence for large-scale glaciation.

It is possible that some of the missing ice volume may have been spread over smaller North American ice masses. For example, the misfit with relative sea-level indicators in the Magdalen Islands (Fig. 8; Pico et al., 2018) hints that ice loading history may be further refined with the addition of MIS 3 ice to the nearby Canadian Appalachians. It is also possible that the northernmost Cordilleran Ice Sheet underwent expansion early in MIS 3 (10Be ages; Ward et al., 2017). However, mountain glaciers hold substantially less ice volume than those on the continent (Tierney et al., 2020), and it is unlikely these regions could hold the missing ~ 30 m of sea-level equivalent implied by the marine $\delta^{18}\text{O}$ record during MIS 3. Additional study of formerly glaciated terrains will provide further refinement of ice loading history across the last glaciation phase. However, the majority of the ~ 30 m discrepancy remains.

Finally, it is possible that ice was growing in the Southern Hemisphere, with the most plausible location being the Antarctic Ice Sheet. However, empirical records from key regions of ice storage do not support ice growth during MIS 3. Instead, available data suggest that the Southern Hemisphere had similar or less ice than today. For example, dating of lacustrine and marine sediments suggest that East Antarctica was ice-free during peak MIS 3 conditions (Berg et al., 2016). Moreover, fossil penguin remains suggest the extent of the Ross Ice Shelf was similar to present during peak MIS 3 (Emslie et al., 2007) and may have only reached its maximum extent around 30 ka (Bart and Cone, 2012). The Indian Ocean sector of the East Antarctic Ice Sheet may have had extra ice volume, which is argued to be necessary to explain MIS 3-aged raised marine deposits (Ishiwa et al., 2021), but the total inferred excess

volume (0.5 m SLE) did not significantly impact global sea level.

5.4. Assessing the feasibility of rapid continental ice advance

Our hypothesis implies dramatic growth and recession of Northern Hemisphere ice masses, notably the Laurentide Ice Sheet over Hudson Bay. Previously it was thought that continental ice sheets need long response periods to retreat and advance. The classic glaciation maps for northern Europe depict gradual growth in the Fennoscandian Ice Sheet over several tens of thousands of years, starting in MIS 4 and culminating in the last glacial maximum (Donner, 1995; Kleman et al., 1997; Lundqvist, 1992; Mangerud, 1991). However, improvements to geochronology and ice sheet modelling indicate a more sensitive response to climate variability. Extensive ice-free areas over central Fennoscandia are reconstructed for late MIS 3 prior to ca. 30 kyr BP based on ^{14}C -dated mammoth remains from Finland and Sweden (Ukkonen et al., 2007; Ukkonen et al., 1999); ice subsequently expanded to a maximum LGM-position on the northern Russian Plain within a timeframe of only 10 kyr (Lunkka et al., 2001).

We also provide two examples of rapid glacier growth from North America. In the west, ice expanded from mountain source areas 250 km from the LGM limit after 19.5 ka (Hicock et al., 1982). Only about 4 kyr later, the Cordilleran Ice Sheet achieved its maximum extent. A second North American example is the rapid advance of the Labrador Dome over Hudson Bay and to the Great Lakes around 38 ka, associated with Heinrich Event 4 (Hemming, 2004). At that time, ice likely advanced over Lake Michigan (between 39.1 and 30.4 ka; Carlson et al., 2018) and potentially to almost the LGM limit in some areas south of the Great Lakes (optically stimulated luminescence dating of proglacial lake

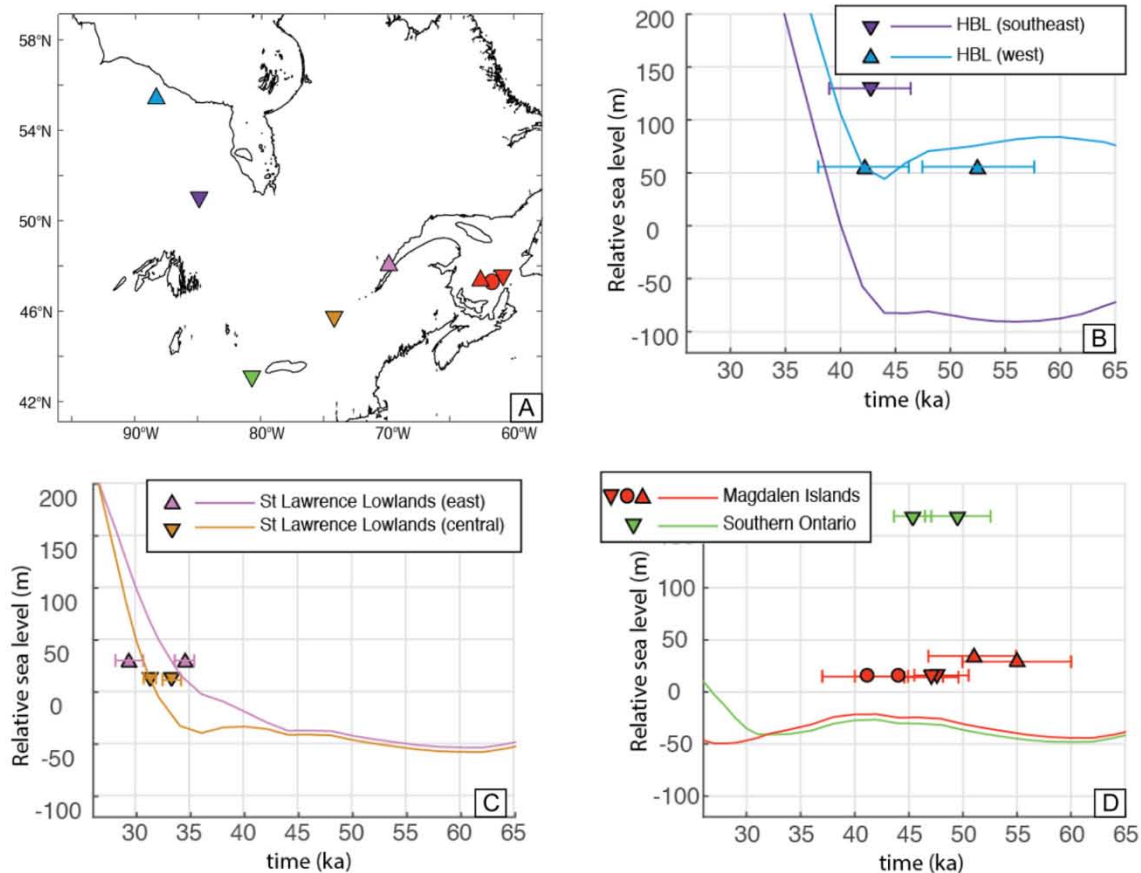


Fig. 8. Locations of marine deposits dated to MIS 3 in eastern North America and their fit to an ice history (ICE-PC2) characterized by a lack of ice over eastern Canada, including the Hudson Bay Lowlands, and a rapid growth in eastern Laurentide ice volume during MIS 3 (modified from Pico et al., 2018). Panels B, C and D show regional relative sea level measurements.

sediments; Wood et al., 2010). This was not a small-scale extension of the ice margin, rather it was a rapid, large-scale advance of >700 km southward in the matter of a few millennia (Carlson et al., 2018). A simple dynamic ice sheet modelling study found that, using accumulation rates similar to that of the present-day Arctic, rapid glaciation rates starting at mid-MIS 3 (44 ka) are predicted, and are sufficient to achieve LGM ice volumes (Pico et al., 2018). Using an idealized model setup, Ji et al. (2021) demonstrated that the merger of two ice domes such as within Hudson Bay would lead to a rapid buildup of ice due to a positive feedback when the ice surface reached above the equilibrium line over a wide area. Thus, we consider the rapid growth and retreat of the Laurentide Ice Sheet during MIS 3 to be feasible. Rapid ice retreat is also possible based on recent empirical and numerical modelling studies that examined post-LGM ice retreat (e.g. possible retreat rates of >1000 km over several 1000s years; Ullman et al., 2015).

The Fennoscandian ice masses were considerably smaller during MIS 3 compared to the Laurentide, but also underwent rapid advance and retreat. Greatly reduced and variable Fennoscandian ice sheet configurations during MIS 5 (~130 ka to 71 ka) and MIS 3 are recorded by the Sokli record and ascribed to enhanced high-latitude insolation values during the warm stages of MIS 5 and early MIS 3 compared to present (Fig. 3). Moreover, there are almost continuous series of optically stimulated luminescence records both from southern Finnish Lapland and central Lapland covering MIS 5 and MIS 3 (Sarala et al., in review), suggesting that at least the southern parts of northern Finland were mostly ice-free at that time. Instead, in the central and northern parts of the Finnish Lapland ice sheets existed during the late MIS 5 (probably during MIS 5b at ~87 ka) and MIS 3, but the stadial phases seemed to be relatively short. Furthermore, there is evidence that northern Finland have been ice free still during 25 ka to 22 ka ago (Sarala et al., 2010). This analysis indicates that stadial stages were relatively short and Fennoscandia glaciers were highly responsive to summer temperature variability during the last glacial cycle.

5.5. Factors that influence the marine $\delta^{18}\text{O}$ record and estimates of continental ice

The marine $\delta^{18}\text{O}$ record is commonly used as a proxy for continental ice volume changes during the Quaternary (sometimes with caveats including corrections for temperature; Bintanja et al., 2005; Govin et al., 2015). However, for early periods of the Cenozoic when continental ice sheets were largely absent, the marine $\delta^{18}\text{O}$ record is used to deduce changes in ocean water temperatures (e.g. Zachos et al., 2001). Disentangling the two main driving parameters in the marine $\delta^{18}\text{O}$ record – temperature and ice volume – is a complicated task. In the early days of interpretation of these data, Shackleton (1967) suggested there was an ice volume component in addition to the known temperature component (Emiliani, 1966). In later work, the additional influence of benthic ocean temperature changes on the $\delta^{18}\text{O}$ record was discussed (Chappell and Shackleton, 1986; Shackleton, 1987). More recently, Lisiecki and Raymo (2005) acknowledged these issues in the widely used global benthic stack.

Several attempts have been made to extract a more accurate ice volume signal from the marine $\delta^{18}\text{O}$ record. Linsley (1996) presented a high-resolution $\delta^{18}\text{O}$ record from the Sulu Sea, western Pacific Ocean, showing significantly different $\delta^{18}\text{O}$ values for MIS 3 than the global stack of Martinson et al. (1987). This discrepancy is ascribed to the semi-isolated configuration of the Sulu Sea basin, insulating the Sulu Sea from oceanographic changes, thus preserving the ice volume signal (Linsley, 1996). Acknowledging the multiple signals of the marine $\delta^{18}\text{O}$ record, Bintanja et al. (2005) took a modelling approach to try to extract the ice volume signal. By integrating continental ice extent and ocean temperatures with the global $\delta^{18}\text{O}$ stack of Lisiecki and Raymo (2005), the authors concluded the impact of continental ice sheets accounted for 10–60% of variation in the marine $\delta^{18}\text{O}$ record. Shakun et al. (2015) also attempt to disentangle the ice volume and temperature signals and

suggest a greater influence of temperature in the early part of glacial cycle. Our findings potentially support the work of Shakun et al. (2015), and would shift estimates for global ice volume from the marine $\delta^{18}\text{O}$ record toward higher GMSL. Foraminiferal diagenesis has been identified as a potential source of isotopic bias in ocean records (Poirier et al., 2021). In sum, our work builds upon previous efforts to separate the two main driving parameters in the marine $\delta^{18}\text{O}$ record (temperature and ice volume) and provides additional empirical evidence in support of these modelling inferences.

As demonstrated in Gowan et al. (2021), part of the discrepancy could derive from the transfer function used to convert from $\delta^{18}\text{O}$ to sea level. Waelbroeck et al. (2002), Shakun et al. (2015) and Spratt and Lisiecki (2016) assume global sea level at the Last Glacial Maximum was ~130 m. However, Simms et al. (2019) suggest that the value may be 18.1 m higher. In Fig. 1, we recalculated sea level using a value of ~111.9 m, which raises sea level during MIS 3 by approximately 10 m in all the records (Gowan et al., 2021). Another explanation could lie in the ocean. Various climate models suggest that even a small change in the height of the ice sheets is sufficient to cause the Atlantic Meridional Overturning Circulation to transition to a weak mode (Obase and Abe-Ouchi, 2019; Peltier and Vettoretti, 2014; Zhang et al., 2014). Thus, under unknown (or unstable) ocean circulation conditions, deep ocean water may not have been well mixed. Further investigating these issues is critical for uncovering the reason behind the ~30 m discrepancy during MIS 3.

It should be noted that the discrepancy between the marine and land-based records concerning global ice volume changes is not restricted to MIS 3. The long late Quaternary sediment record preserved at Sokli in the central area of Fennoscandian glaciation shows that interglacial conditions, with a vegetation and climate comparable to the Holocene, not only prevailed during MIS 5e (~123 ka) but also occurred during MIS 5c (~96 ka) and MIS 5a (~82 ka; Fig. 3), precluding the presence of any significant ice mass in Fennoscandia during at these times. This is in disagreement with the $\delta^{18}\text{O}$ record that suggests enhanced ice volumes during MIS 5c and 5a compared to the Holocene, but in agreement with data from tectonically stable locations indicating a sea-level highstand comparable to today during MIS 5a (Dorale et al., 2010). Glacial isostatic adjustment modelling results for these times also suggest that sea level was higher than predicted from the $\delta^{18}\text{O}$ record (Creveling et al., 2017). The warm conditions at Sokli during the warm stages of MIS 5 and early MIS 3 (Fig. 3) are ascribed to increased high-latitude insolation values during these periods compared to present (Fig. 3).

5.6. Obtaining sea level estimates from corals

One source of validation of the $\delta^{18}\text{O}$ record is the Huon Peninsula (Papua New Guinea) coral terrace sequence (Chappell et al., 1996; Waelbroeck et al., 2002). Interestingly, early dating attempts at that site using alpha-spectrometry suggested that the inferred sea level during MIS 3 (after correcting for the uplift rate) was ~30 to ~70 m, which aligns with our hypothesis. Chappell et al. (1996) employed more precise thermal ion mass spectrometry measurements that led to the same terrace being determined to be older, and as a result the inferred sea level estimate was 20–40 m lower, providing a reconciliation between the sea level estimates and inferences from the $\delta^{18}\text{O}$ record.

Some more recent work presents an alternative interpretations of the data at Huon Peninsula, which aligns more closely with our hypothesis. Hibbert et al. (2016) created a database of sea level indicators from corals, recalculated their ages, and reassessed the vertical uncertainties using the modern depth range of coral species. Their analysis showed a potential sea level estimate ten of meters higher than the median estimate. The uncertainty range derived using the modern depth range may overestimate the true water depth that can be inferred from an in-situ coral if other geological evidence is present to provide support for a shallower depth (e.g. through coral assemblages; Chutcharavan and Dutton, 2020). The tectonic uplift rate is complicated in the Huon

Peninsula because it is spatially variable. Using a high resolution digital elevation model, de Gelder et al. (2021) calculated the uplift rate from the MIS 5e reef across the Huon Peninsula, and used that to estimate the MIS 3 highstand position. They found that the reevaluated uplift rates would raise the estimated sea level during MIS 3 by 3–10 m. These factors demonstrate the difficulty of using sea level estimates from corals, especially in rapidly uplifting regions, and highlight the care that must be taken when interpreting them.

6. Conclusion

The accumulating geological data from the glaciated region of the Northern Hemisphere, along with glacial isostatic adjustment modelling, summarized herein, are in opposition to large ice sheets during MIS 3 as deduced from the relatively enriched marine $\delta^{18}\text{O}$ values in the global stack. Although some geochronological data are vulnerable to misinterpretation (especially radiocarbon ages near the limit of reliability for that method) the ensemble of evidence pointing to significantly reduced ice volumes during MIS 3, following MIS 4 deglaciation, cannot be ignored. This work urges caution regarding the reliance of the marine $\delta^{18}\text{O}$ record as a de facto indicator of continental ice during times when few geological constraints are available, which underpins many Quaternary studies.

Declaration of Competing Interest

The authors declare that they have no known competing financial interests or personal relationships that could have appeared to influence the work reported in this paper.

Acknowledgments

T.P. acknowledges funding from an NSF-EAR Postdoctoral Fellowship and UC President's Postdoc Program Fellowship. Field work in northern Hudson Bay (Nunavut) is a contribution to Natural Resources Canada Geomapping for Energy and Minerals (GEM) Program (NRCan contribution number 20210064). E.J.G. was funded by Impuls- und Vernetzungsfonds, Helmholtz-Exzellenznetzwerke (grant no. ExNet-0001-Phase 2-3) "The Polar System and its Effects on the Ocean Floor (POSY)", Helmholtz Climate Initiative REKLIM (Regional Climate Change), a joint research project at the Helmholtz Association of German research centers (HGF), the PACES-II program at the Alfred Wegener Institute and the Bundesministerium für Bildung und Forschung funded project, PalMod, and a Japan Society for the Promotion of Science International Postdoctoral Research Fellowship. K.F.H. acknowledges funding from the Swedish Nuclear Fuel and Waste Management Company (SKB). The authors acknowledge PALSEA, a working group of the International Union for Quaternary Sciences (INQUA) and Past Global Changes (PAGES), which in turn received support from the Swiss Academy of Sciences and the Chinese Academy of Sciences. We thank Martin Roy and Pierre-Marc Godbout for constructive feedback, as well as three anonymous reviewers. Finally, we thank the INQUA Dublin 2019 scientific committee for allowing us to present some aspects of our work in a session entitled: Estimates of Global Ice Volumes During MIS 3 in Need of Re-Evaluation: A Multi-Disciplinary Approach.

Appendix A. Supplementary data

Supplementary data to this article can be found online at <https://doi.org/10.1016/j.gloplacha.2022.103814>.

References

Adkins, J.F., McIntyre, K., Schrag, D.P., 2002. The salinity, temperature, and $\delta^{18}\text{O}$ of the glacial deep ocean. *Science* 298 (5599), 1769–1773.

- Aharon, P., 2003. Meltwater flooding events in the Gulf of Mexico revisited: Implications for rapid climate changes during the last deglaciation. *Paleoceanography* 18 (4), PA000840.
- Alexanderson, H., Johnsen, T., Murray, A.S., 2010. Re-dating the Pilgrim Interstadial with OSL: a warmer climate and smaller ice sheet during the Swedish Middle Weichselian (MIS 3)? *Boreas* 39, 367–376.
- Alexanderson, H., Hättestrand, M., Buylaert, J.P., 2011. New dates from the Riipiharju interstadial site, northernmost Sweden [conference abstract]. In: Late Pleistocene Glacigenic Deposits from the Central Part of the Scandinavian Ice Sheet to Younger Dryas End Moraine Zone, Rovaniemi, Finland, June 12–17, 2011.
- Allard, G., et al., 2012. Constraining the age of the last interglacial–glacial transition in the Hudson Bay lowlands (Canada) using U–Th dating of buried wood. *Quat. Geochronol.* 7, 37–47.
- Alley, N.F., 1979. Middle Wisconsin stratigraphy and climatic reconstruction, southern Vancouver Island, British Columbia. *Quat. Res.* 11 (2), 213–237.
- Andersen, B.G., Mangerud, J., 1989. The last interglacial–glacial cycle in Fennoscandia. *Quat. Int.* 3–4, 21–29.
- Andrews, J.T., Voelker, A.H.L., 2018. "Heinrich events" (& sediments): a history of terminology and recommendations for future usage. *Quat. Sci. Rev.* 187, 31–40.
- Andrews, J.T., Shilts, W.W., Miller, G.H., 1983. Multiple deglaciations of the Hudson Bay Lowlands, Canada, since deposition of the Missinaibi (Last-Interglacial?) Formation. *Quat. Res.* 19, 13–37.
- Armstrong, J.E., Clague, J.J., 1977. Two major Wisconsin lithostratigraphic units in Southwest British Columbia. *Can. J. Earth Sci.* 14 (7), 1471–1480.
- Armstrong, J.E., Crandell, D.R., Easterbrook, D.J. and Noble, J.B., 1965. Late Pleistocene stratigraphy and chronology in southwestern British Columbia and northwestern Washington. *Geol. Soc. Am. Bull.* 76 (3), 321–330.
- Arnold, N.S., van Andel, T.H., Valen, V., 2002. Extent and dynamics of the Scandinavian Ice Sheet during Oxygen Isotope Stage 3 (65,000–25,000 yr B.P.). *Quat. Res.* 57 (1), 38–48.
- Ballantyne, C.K., Small, D., 2019. The last Scottish ice sheet. *Earth Environ. Sci. Trans. Royal Soc. Edinburgh* 110 (1–2), 93–131.
- Bart, P.J., Cone, A.N., 2012. Early stall of West Antarctic Ice Sheet advance on the eastern Ross Sea middle shelf followed by retreat at 27,500 ^{14}C yr BP. *Palaeogeogr. Palaeoclimatol. Palaeoecol.* 335–336, 52–60.
- Batchelor, C.L., et al., 2019. The configuration of Northern Hemisphere ice sheets through the Quaternary. *Nat. Commun.* 10 (1), 3713.
- Baumann, K.-H., et al., 1995. Reflection of Scandinavian Ice Sheet fluctuations in Norwegian Sea sediments during the past 150,000 years. *Quat. Res.* 43 (2), 185–197.
- Behre, K.-E., van der Plicht, J., 1992. Towards an absolute chronology for the last glacial period in Europe: radiocarbon dates from Oerel, northern Germany. *Veg. Hist. Archaeobotany* 1, 111–117.
- Bélanger, N., Carcaillet, C., Padbury, G.A., Harvey-Schafer, A.N., Van Rees, K.J., 2014. Periglacial fires and trees in a continental setting of Central Canada, Upper Pleistocene. *Geobiology* 12 (2), 109–118.
- Berg, S., et al., 2016. Unglaciated areas in East Antarctica during the last Glacial (Marine Isotope Stage 3) – New evidence from Rauer Group. *Quat. Sci. Rev.* 153, 1–10.
- Berger, A., Loutre, M.F., 1991. Insolation values for the climate of the last 10 million years. *Quat. Sci. Rev.* 10 (4), 297–317.
- Berger, G.W., Nielsen, E., 1990. Evidence from thermoluminescence dating for Middle Wisconsinan deglaciation in the Hudson Bay Lowland of Manitoba. *Can. J. Earth Sci.* 28, 240–249.
- Berger, A., et al., 2016. Interglacials of the last 800,000 years. *Rev. Geophys.* 54 (1), 162–219.
- Bettis, E.A.L., Muhs, D.R., Roberts, H.M., Wintle, A.G., 2003. Last Glacial loess in the conterminous USA. *Quat. Sci. Rev.* 22 (18–19), 1907–1946.
- Bezerra, F.H., Vita-Finzi, C., Filho, F.P.L., 2000. The use of marine shells for radiocarbon dating of coastal deposits. *Brazil. J. Geol.* 30, 211–213.
- Bintanja, R., van de Wal, R.S.W., Oerlemans, J., 2005. Modelled atmospheric temperatures and global sea levels over the past million years. *Nature* 437, 125–128.
- Bond, G., et al., 1993. Correlations between climate records from North Atlantic sediments and Greenland ice. *Nature* 365 (6442), 143–147.
- Bos, J.A.A., Helmens, K., Bohncke, S.J.P., Seppä, H., Birks, H., 2009. Flora, vegetation and climate at Sokli, northern Fennoscandia, during the Weichselian Middle Pleniglacial. *Boreas* 38, 335–348.
- Burns, J.A., 1996. Vertebrate paleontology and the alleged ice-free corridor: the meat of the matter. *Quat. Int.* 32, 107–112.
- Carlson, A.E., Tarasov, L., Pico, T., 2018. Rapid Laurentide ice-sheet advance towards southern last glacial maximum limit during marine isotope stage 3. *Quat. Sci. Rev.* 196, 118–123.
- Ceperley, E.G., Marcott, S.A., Rawling, J.E., Zoet, L.K., Zimmerman, S.R.H., 2019. The role of permafrost on the morphology of an MIS 3 moraine from the southern Laurentide Ice Sheet. *Geology* 47 (5), 440–444.
- Chappell, J., 2002. Sea level changes forced ice breakouts in the last Glacial cycle: new results from coral terraces. *Quat. Sci. Rev.* 21 (10), 1229–1240.
- Chappell, J., Shackleton, N.J., 1986. Oxygen isotopes and sea level. *Nature* 324 (6093), 137–140.
- Chappell, J., et al., 1996. Reconciliation of late Quaternary Sea levels derived from coral terraces at Huon Peninsula with deep sea oxygen isotope records. *Earth Planet. Sci. Lett.* 141 (1), 227–236.
- Chutcharavan, P.M., Dutton, A., 2020. A global compilation of u-series dated fossil coral sea-level indicators for the last interglacial period (MIS 5e). *Earth Syst. Sci. Data Discuss.* 2020, 1–41.
- Clague, J.J., 1981. Late Quaternary geology and geochronology of British Columbia, part 2: summary and discussion of radiocarbon-dated quaternary history. *Geol. Surv. Can. Pap.* 80–35 1–41.

- Clague, J.J., Hebda, R.J., Mathewes, R.W., 1990. Stratigraphy and paleoecology of Pleistocene interstadial sediments, Central British Columbia. *Quat. Res.* 34 (2), 208–226.
- Clark, P.U., et al., 2009. The last Glacial Maximum. *Science* 325 (5941), 710–714.
- Creveling, J.R., Mitrovica, J.X., Clark, P.U., Waelbroeck, C., Pico, T., 2017. Predicted bounds on peak global mean sea level during marine isotope stages 5a and 5c. *Quat. Sci. Rev.* 163, 193–208.
- Dalton, A.S., Finkelstein, S.A., Barnett, P.J., Forman, S.L., 2016. Constraining the late Pleistocene history of the Laurentide Ice Sheet by dating the Missinaibi Formation, Hudson Bay Lowlands, Canada. *Quat. Sci. Rev.* 146, 288–299.
- Dalton, A.S., Väiranta, M., Barnett, P.J., Finkelstein, S.A., 2017. Pollen and macrofossil-inferred paleoclimate at the Ridge Site, Hudson Bay Lowlands, Canada: evidence for a dry climate and significant recession of the Laurentide Ice Sheet during Marine Isotope Stage 3. *Boreas* 46 (3), 388–401.
- Dalton, A.S., Finkelstein, S.A., Barnett, P.J., Väiranta, M., Forman, S.L., 2018. Late Pleistocene chronology, paleoecology and stratigraphy at a suite of sites along the Albany River, Hudson Bay Lowlands, Canada. *Palaeogeogr. Palaeoclimatol. Palaeoecol.* 492, 50–63.
- Dalton, A.S., et al., 2019. Was the Laurentide Ice Sheet significantly reduced during Marine Isotope Stage 3? *Geology* 47 (2), 111–114.
- Dalton, A.S., Stokes, C.R., Batchelor, C.L., 2022. Evolution of the Laurentide and Innuitian ice sheets prior to the last Glacial Maximum (115 ka to 25 ka). *Earth Sci. Rev.* 224, 103875.
- Dansgaard, W., et al., 1993. Evidence for general instability of past climate from a 250-kyr ice-core record. *Nature* 364, 218–220.
- De Boer, B., Stocchi, P., Wal, R.S.W., 2014. A fully coupled 3-D ice-sheet-sea-level model: algorithm and applications. *Geosci. Model Dev.* 7.
- de Gelder, G., et al., 2021. High interstadial sea levels over the past 420ka from Huon terraces (Papua New Guinea) [Preprint on EarthArXiv] doi: 10.31223/X5C03Z.
- Dendy, S.N., Guenther, W.R., Grimley, D.A., Conroy, J.L., Counts, R.C., 2021. Detrital zircon geochronology and provenance of Pleistocene loess and contributing glacial sources, midcontinental USA. *Quat. Sci. Rev.* 273, 107201.
- Donner, J., 1995. The Quaternary History of Scandinavia. *World and Regional Geology*, 7. Cambridge University Press, p. 200.
- Dorale, J.A., Edwards, R.L., Ito, E., González, L.A., 1998. Climate and vegetation history of the midcontinent from 75 to 25 ka: a speleothem record from Crevice Cave, Missouri, USA. *Science* 282 (5395), 1871–1874.
- Dorale, J.A., et al., 2010. Sea-level highstand 81,000 years ago in Mallorca. *Science* 327, 860–863.
- Douka, K., Hedges, R.E.M., Higham, T.F.G., 2010a. Improved AMS 14C dating of shell carbonates using high-precision X-Ray diffraction and a novel density separation protocol (Cards). *Radiocarbon* 52 (2), 735–751.
- Douka, K., Higham, T.F.G., Hedges, R.E.M., 2010b. Radiocarbon dating of shell carbonates: old problems and new solutions. *Munibe Supplement*, 31, 18–27.
- Dredge, L.A., Thorleifson, L.H., 1987. The Middle Wisconsinan history of the Laurentide Ice Sheet. *Geol. Phys. Quatern.* 41 (2), 215–235.
- Dubé-Loubert, H., Roy, M., Allard, G., Lamothe, M., Veillette, J.J., 2013. Glacial and nonglacial events in the eastern James Bay lowlands, Canada. *Can. J. Earth Sci.* 50 (4), 379–396.
- Dyke, A.S., et al., 2002. The Laurentide and Innuitian ice sheets during the last Glacial Maximum. *Quat. Sci. Rev.* 21 (1–3), 9–31.
- Elderfield, H., et al., 2012. Evolution of Ocean Temperature and Ice volume through the Mid-Pleistocene climate transition. *Science* 337 (6095), 704–709.
- Emilian, C., 1966. Isotopic Paleotemperatures: Urey's method of paleotemperature analysis has greatly contributed to our knowledge of past climates. *Science* 154 (3751), 851–857.
- Emslie, S.D., Coats, L., Licht, K., 2007. A 45,000 yr record of Adélie penguins and climate change in the Ross Sea, Antarctica. *Geology* 35 (1), 61–64.
- Engels, S., et al., 2008. Chironomid-based paleotemperature estimates for Northeast Finland during Oxygen Isotope Stage 3. *J. Paleolimnol.* 40 (1), 49–61.
- Fischer, H., et al., 2015. Millennial changes in north American wildfire and soil activity over the last glacial cycle. *Nat. Geosci.* 8 (9), 723–727.
- Flint, R.F., 1943. Growth of north American ice sheet during the Wisconsin age. *Geol. Soc. Am. Bull.* 54 (3), 325–362.
- Flower, B.P., Williams, C., Hill, H.W., Hastings, D.W., 2011. Laurentide Ice Sheet meltwater and the Atlantic Meridional Overturning Circulation during the last glacial cycle: a view from the Gulf of Mexico. In: *Abrupt Climate Change: Mechanisms, Patterns, and Impacts*. American Geophysical Union, Washington, D.C.
- Follmer, L.R., 1996. Loess studies in Central United States: evolution of concepts. *Eng. Geol.* 45 (1), 287–304.
- Forman, S.L., Pierson, J., 2002. Late Pleistocene luminescence chronology of loess deposition in the Missouri and Mississippi river valleys, United States. *Palaeogeogr. Palaeoclimatol. Palaeoecol.* 186, 25–46.
- Forman, S.L., Wintle, A.G., Thorleifson, L.H., Wyatt, P.H., 1987. Thermoluminescence properties and age estimates for Quaternary raised marine sediments, Hudson Bay Lowland, Canada. *Can. J. Earth Sci.* 24, 2405–2411.
- Fox-Kemper, B., et al., 2021. Ocean, Cryosphere and Sea Level Change. In: *Climate Change 2021: The Physical Science Basis. Contribution of Working Group I to the Sixth Assessment Report of the Intergovernmental Panel on Climate Change*. Cambridge University Press.
- Fulton, R.J., 1968. Olympia Interglaciation, Purcell Trench, British Columbia. *Geol. Soc. Am. Bull.* 79 (8), 1075–1080.
- Fulton, R.J., Smith, G.W., 1978. Late Pleistocene stratigraphy of south-Central British Columbia. *Can. J. Earth Sci.* 15 (6), 971–980.
- Gauthier, M.S., Hodder, T.J., 2020. Surficial geology mapping from Manigotagan to Berens River, southeastern Manitoba (parts of NTS 62P1, 7, 8, 10, 15, 63A2, 7). In: *Report of Activities 2020, Manitoba Agriculture and Resource Development, Manitoba Geological Survey*, pp. 41–46.
- Gauthier, M.S., et al., 2019. The subglacial mosaic of the Laurentide Ice Sheet: a study of the interior region of southwestern Hudson Bay. *Quat. Sci. Rev.* 214, 1–27.
- Govin, A., et al., 2015. Sequence of events from the onset to the demise of the last Interglacial: evaluating strengths and limitations of chronologies used in climatic archives. *Quat. Sci. Rev.* 129, 1–36.
- Gowan, E.J., et al., 2021. Global ice sheet reconstruction for the past 80000 years. *Nat. Commun.* 12 (1199).
- Grant, K.M., et al., 2014. Sea-level variability over five glacial cycles. *Nat. Commun.* 5, 5076.
- Harrington, C.R., Tipper, H.W., Mott, R.J., 1974. Mammoth from Babine Lake, British Columbia. *Can. J. Earth Sci.* 11 (2), 285–303.
- Hastings, D.W., Russell, A.D., Emerson, S.R., 1998. Foraminiferal magnesium in *Globeriginoides sacculifer* as a paleotemperature proxy. *Paleoceanography* 13 (2), 161–169.
- Hättestrand, M., Robertson, A.-M., 2010. Weichselian interstadials at Riipiharju, northern Sweden – interpretation of vegetation and climate from fossil and modern pollen records. *Boreas* 39, 296–311.
- Heaton, T.J., et al., 2020. Marine20—the marine radiocarbon age calibration curve (0–55,000 cal BP). *Radiocarbon* 62 (4), 779–820.
- Hebda, R.J., Lian, O.B., Hicock, S.R., Fisher, T.G., 2016. Olympia Interstadial: vegetation, landscape history, and paleoclimatic implications of a mid-Wisconsinan (MIS3) nonglacial sequence from Southwest British Columbia, Canada. *Can. J. Earth Sci.* 53 (3), 304–320.
- Helmens, K.F., 2014. The Last Interglacial–Glacial cycle (MIS 5–2) re-examined based on long proxy records from central and northern Europe. *Quat. Sci. Rev.* 86, 115–143.
- Helmens, K.F., et al., 2007. Present-day temperatures in northern Scandinavia during the last glaciation. *Geology* 35 (11), 987–990.
- Helmens, K.F., et al., 2009. Early MIS 3 glacial lake evolution, ice-marginal retreat pattern and climate at Sokli (northeastern Fennoscandia). *Quat. Sci. Rev.* 28 (19), 1880–1894.
- Helmens, K.F., et al., 2018. Warm summers and rich biotic communities during N-Hemisphere deglaciation. *Glob. Planet. Chang.* 167, 61–73.
- Helmens, K.F., et al., 2021. Prolonged interglacial warmth during the last Glacial in northern Europe. *Boreas* 50 (2), 331–350.
- Hemming, S.R., 2004. Heinrich events: massive late Pleistocene detritus layers of the North Atlantic and their global climate imprint. *Rev. Geophys.* 42(1), RG1005, 1–43.
- Herring, E.M., Gavin, D.G., 2015. Climate and vegetation since the last Interglacial (MIS 5e) in a putative glacial refugium, northern Idaho, USA. *Quat. Sci. Rev.* 117, 82–95.
- Hibbert, F.D., et al., 2016. Coral indicators of past sea-level change: a global repository of U-series dated benchmarks. *Quat. Sci. Rev.* 145, 1–56.
- Hickin, A.S., Lian, O.B., Levson, V.M., 2016. Coalescence of late Wisconsinan Cordilleran and Laurentide ice sheets east of the Rocky Mountain Foothills in the Dawson Creek region, Northeast British Columbia, Canada. *Quat. Res.* 85 (3), 409–429.
- Hicock, S.R., Hebda, R.J., Armstrong, J.E., 1982. Lag of the Fraser glacial maximum in the Pacific Northwest: pollen and macrofossil evidence from western Fraser Lowland, British Columbia. *Can. J. Earth Sci.* 19 (12), 2288–2296.
- Hirvas, H., 1991. Pleistocene stratigraphy of Finnish Lapland. *Geol. Survey Finland Bull.* 354, 123.
- Houmark-Nielsen, M., Kjær, K.H., 2003. Southwest Scandinavia, 40–15 kyr BP: palaeogeography and environmental change. *J. Quat. Sci.* 18, 1–18.
- Howett, P.J., Salonen, V.-P., Hyttinen, O., Korkka-Niemi, K., Moreau, J., 2015. A hydrostratigraphical approach to support environmentally safe siting of a mining waste facility at Rautuvaara, Finland. *Bull. Geol. Soc. Finl.* 87, 51–66.
- Hughes, A.L.C., Gyllencreutz, R., Lohne, Ø.S., Mangerud, J., Svendsen, J.I., 2016. The Last Eurasian ice sheets – a chronological database and time-slice reconstruction, DATED-1. *Boreas* 45, 1–45.
- Ishiya, T., Okuno, J.I., Suganuma, Y., 2021. Excess ice loads in the Indian Ocean sector of East Antarctica during the last glacial period. *Geology* 49 (10), 1182–1186.
- Ivester, A.H., Leigh, D.S., Godfrey-Smith, D.I., 2001. Chronology of inland eolian dunes on the coastal plain of Georgia, USA. *Quat. Res.* 55 (3), 293–302.
- Ji, W., Robel, A., Tziperman, E., Yang, J., 2021. Laurentide Ice Saddle Mergers Drive Rapid Sea Level Drops during Glaciations. *Geophys. Res. Lett.* 48 (14), e2021GL094263.
- Johansson, P., Lunkka, J.P., Sarala, P., 2011. Chapter 9 - the glaciation of Finland. In: *Ehlers, J., Gibbard, P.L., Hughes, P.D. (Eds.), Developments in Quaternary Sciences*. Elsevier, pp. 105–116.
- Johnsen, S.J., et al., 1992. Irregular glacial interstadials recorded in a new Greenland ice core. *Nature* 359, 311–313.
- Kerr, P.J., et al., 2021. Timing, provenance, and implications of two MIS 3 advances of the Laurentide Ice Sheet into the Upper Mississippi River Basin, USA. *Quat. Sci. Rev.* 261, 106926.
- Kleman, J., Hättestrand, C., Borgström, I., Stroeve, A., 1997. Fennoscandian palaeoglaciology reconstructed using a glacial geological inversion model. *J. Glaciol.* 43 (144), 283–299.
- Kleman, J., Hättestrand, M., Borgström, I., Preusser, F., Fabel, D., 2020. The Idre marginal moraine – an anchorpoint for Middle and late Weichselian ice sheet chronology. *Quat. Sci. Adv.* 2.
- Larsen, E., et al., 2006. Late Pleistocene glacial and lake history of northwestern Russia. *Boreas* 35 (3), 394–424.
- Lea, D.W., Pak, D.K., Spero, H.J., 2000. Climate impact of late quaternary equatorial Pacific Sea surface temperature variations. *Science* 289 (5485), 1719.
- Leigh, D.S., 1994. Roxana silt of the Upper Mississippi Valley: Lithology, source and paleoenvironment. *Geol. Soc. Am. Bull.* 106, 430–442.

- Leigh, D., Srivastava, P., Brook, G., 2004. Late Pleistocene braided rivers of the Atlantic Coastal Plain, USA. *Quat. Sci. Rev.* 23 (1–2), 65–84.
- Linsley, B.K., 1996. Oxygen-isotope record of sea level and climate variations in the Sulu Sea over the past 150,000 years. *Nature* 380 (6571), 234–237.
- Lisiecki, L.E., Raymo, M.E., 2005. A Pliocene-Pleistocene stack of 57 globally distributed benthic $\delta^{18}\text{O}$ records. *Paleoceanography* 20 (1).
- Lundqvist, J., 1992. Glacial stratigraphy in Sweden. In: Kauranne, K. (Ed.), *Glacial Stratigraphy, Engineering Geology and Earth Construction: Geological Survey of Finland, Special Paper 15*, pp. 43–59.
- Lunkka, J.P., Saarnisto, M., Gey, V., Demidov, I., Kiselova, V., 2001. Extent and age of the Last Glacial Maximum in the southeastern sector of the Scandinavian Ice Sheet. *Glob. Planet. Chang.* 31 (1), 407–425.
- Lunkka, J.P., Murray, A., Korpela, K., 2008. Weichselian sediment succession at Ruunaa, Finland, indicating a Mid-Weichselian ice-free interval in eastern Fennoscandia. *Boreas* 37 (2), 234–244.
- Lunkka, J.P., Sarala, P., Gibbard, P.L., 2015. The Rautuvaara section, western Finnish Lapland, revisited – new age constraints indicate a complex Scandinavian Ice Sheet history in northern Fennoscandia during the Weichselian Stage. *Boreas* 44 (1), 68–80.
- Mäkinen, K., 2005. Dating the Weichselian deposits of southwestern Finnish Lapland. *Geol. Surv. Finland Spec. Pap.* 40, 67–78.
- Mangerud, J., 1991. The Scandinavian Ice Sheet through the last interglacial/glacial cycle. In: Frenzel, B. (Ed.), *Klimageschichtliche Probleme der letzten 130 000 Jahre*. Stuttgart, pp. 307–330.
- Mangerud, J., Gulliksen, S., Larsen, E., 2010. ^{14}C -dated fluctuations of the western flank of the Scandinavian Ice Sheet 45–25 kyr BP compared with Bølling–Younger Dryas fluctuations and Dansgaard–Oeschger events in Greenland. *Boreas* 39 (2), 328–342.
- Margold, M., Stokes, C.R., Clark, C.D., 2015. Ice streams in the Laurentide Ice Sheet: Identification, characteristics and comparison to modern ice sheets. *Earth Sci. Rev.* 143, 117–146.
- Martinson, D.G., et al., 1987. Age Dating and the orbital theory of the Ice Ages: Development of a high-resolution 0 to 300,000-year chronostratigraphy. *Quat. Res.* 27 (1), 1–29.
- Mathewes, R.W., Richards, M., Reimchen, T.E., 2019. Late Pleistocene age, size, and paleoenvironment of a caribou antler from Haida Gwaii, British Columbia. *Can. J. Earth Sci.* 56 (6), 688–692.
- McManus, J.F., et al., 1994. High-resolution climate records from the North Atlantic during the last interglacial. *Nature* 371 (6495), 326–329.
- McMartin, I., Campbell, J.E., Dredge, L.A., 2019. Middle Wisconsinan marine shells near Repulse Bay, Nunavut, Canada: implications for Marine Isotope Stage 3 ice-free conditions and Laurentide Ice Sheet dynamics in north-West Hudson Bay. *J. Quat. Sci.* 34 (1), 64–75.
- McMartin, I., Godbout, P.-M., Campbell, J.E., Tremblay, T., Behnia, P., 2021. A new map of glacial features and glacial landsystems in central mainland Nunavut, Canada. *Boreas* 50 (1), 51–75.
- Miller, G.H., Andrews, J.T., 2019. Hudson Bay was not deglaciated during MIS-3. *Quat. Sci. Rev.* 225, 105944.
- Möller, P., Anjar, J., Murray, A.S., 2013. An OSL-dated sediment sequence at Idre, west-Central Sweden, indicates ice-free conditions in MIS 3. *Boreas* 42 (1), 25–42.
- Möller, P., Alexanderson, H., Anjar, J., Björck, S., 2020. MIS 3 sediment stratigraphy in southern Sweden sheds new light on the complex glacial history and dynamics across southern Scandinavia. *Boreas* 49 (3), 389–416.
- Nishizawa, S., Currey, D.R., Brunelle, A., Sack, D., 2013. Bonneville basin shoreline records of large lake intervals during Marine Isotope Stage 3 and the Last Glacial Maximum. *Palaeogeogr. Palaeoclimatol. Palaeoecol.* 386, 374–391.
- Obase, T., Abe-Ouchi, A., 2019. Abrupt boiling-allered warming simulated under gradual forcing of the last deglaciation. *Geophys. Res. Lett.* 46 (20), 11397–11405.
- Olsen, L., et al., 2001a. Methods and stratigraphies used to reconstruct Mid- and Late Weichselian palaeoenvironmental and paleoclimatic changes in Norway. *Norges Geologisk Undersøgelse Bull.* 438, 21–46.
- Olsen, L.O., et al., 2001b. AMS radiocarbon dating of glacial sediments with low organic carbon content – an important tool for reconstructing the history of glacial variations in Norway. *Nor. J. Geol.* 81, 59–92.
- Paus, A., Velle, G., Berge, J., 2011. The Lateglacial and early Holocene vegetation and environment in the Dovre mountains, Central Norway, as signalled in two Lateglacial nunatak lakes. *Quat. Sci. Rev.* 30 (13), 1780–1796.
- Peltier, W.R., Vettoretti, G., 2014. Dansgaard–Oeschger oscillations predicted in a comprehensive model of glacial climate: a “kicked” salt oscillator in the Atlantic. *Geophys. Res. Lett.* 41 (20), 7306–7313.
- Pico, T., Mitrovica, J.X., Ferrier, K.L., Braun, J., 2016. Global ice volume during MIS 3 inferred from a sea-level analysis of sedimentary core records in the Yellow River Delta. *Quat. Sci. Rev.* 152, 72–79.
- Pico, T., Creveling, J.R., Mitrovica, J.X., 2017. Sea-level records from the U.S. mid-Atlantic constrain Laurentide Ice Sheet extent during Marine Isotope Stage 3. *Nat. Commun.* 8, 15612.
- Pico, T., Birch, L., Weisenberg, J., Mitrovica, J.X., 2018. Refining the Laurentide Ice Sheet at Marine Isotope Stage 3: a data-based approach combining glacial isostatic simulations with a dynamic ice model. *Quat. Sci. Rev.* 195, 171–179.
- Poirier, R.K., et al., 2021. Quantifying diagenesis, contributing factors, and resulting isotopic bias in benthic foraminifera using the foraminiferal preservation index: implications for geochemical proxy records. *Paleoceanogr. Paleoclimatol.* 36 (5), e2020PA004110.
- Reimer, P.J., et al., 2020. The IntCal20 Northern Hemisphere radiocarbon age calibration curve (0–55 cal kBP). *Radiocarbon* 62 (4), 725–757.
- Salonen, V.-P., et al., 2008. Middle Weichselian glacial event in the central part of the Scandinavian Ice Sheet recorded in the Hitura pit, Ostrobothnia, Finland. *Boreas* 37 (1), 38–54.
- Salonen, V.-P., Moreau, J., Hyttinen, O., Eskola, K.O., 2014. Mid-Weichselian interstadial in Kolari, western Finnish Lapland. *Boreas* 43 (3), 627–638.
- Salonen, J.S., et al., 2018. Abrupt high-latitude climate events and decoupled seasonal trends during the Eemian. *Nat. Commun.* 9 (1), 2851.
- Sarala, P., 2005. Weichselian stratigraphy, geomorphology and glacial dynamics in southern Finnish Lapland. *Bull. Geol. Soc. Finl.* 77, 71–104.
- Sarala, P., 2019. Evidence of Long Ice-Free Conditions during MIS 3 in Northern Finland [abstract] 20th INQUA Congress, Dublin, Ireland 25–31 July 2019. <https://app.oxfordabstracts.com/events/574/program-app/submission/92625>.
- Sarala, P., Eskola, T., 2011. Middle Weichselian interstadial deposit at Petäjäselkä, Northern Finland. *E & G Quat. Sci. J.* 60 (4), 488–492.
- Sarala, P., Lunkka, J.P., Sarajärvi, V., Sarala, O. and Filzmoser, P., in review. Variation of glacial – ice-free stages in Finland with an exploratory analysis of the OSL age data. *Arctic, Antarctic and Alpine Research*.
- Sarala, P., Pihlaja, J., Putkinen, N., Murray, A., 2010. Composition and origin of the Middle Weichselian interstadial deposit in Veskonieni, northern Finland. *Estonian J. Earth Sci.* 59 (2), 117–124.
- Sarala, P., Väilänta, M., Eskola, T., Vaikutene, G., 2016. First physical evidence for forested environment in the Arctic during MIS 3. *Sci. Rep.* 6, 29054.
- Schrag, D.P., Hampt, G., Murray, D.W., 1996. Pore Fluid Constraints on the Temperature and Oxygen Isotopic Composition of the Glacial Ocean. *Science* 272 (5270), 1930–1932.
- Seguinot, J., Rogozhina, I., Stroeve, A.P., Margold, M., Kleman, J., 2016. Numerical simulations of the Cordilleran ice sheet through the last glacial cycle. *Cryosphere* 10 (2), 639–664.
- Shackleton, N., 1967. Oxygen Isotope analyses and Pleistocene Temperatures Re-assessed. *Nature* 215 (5096), 15–17.
- Shackleton, N.J., 1987. Oxygen isotopes, ice volume and sea level. *Quat. Sci. Rev.* 6 (3), 183–190.
- Shakun, J.D., Lea, D.W., Lisiecki, L.E., Raymo, M.E., 2015. An 800-kyr record of global surface ocean $\delta^{18}\text{O}$ and implications for ice volume-temperature coupling. *Earth Planet. Sci. Lett.* 426, 58–68.
- Siddall, M., Rohling, E.J., Thompson, W.G., Waelbroeck, C., 2008. Marine Isotope Stage 3 sea level fluctuations: Data synthesis and new outlook. *Rev. Geophys.* 46 (4), RG4003.
- Simms, A.R., Lisiecki, L., Gebbie, G., Whitehouse, P.L., Clark, J.F., 2019. Balancing the last glacial maximum (LGM) sea-level budget. *Quat. Sci. Rev.* 205, 143–153.
- Sionneau, T., et al., 2013. Atmospheric re-organization during Marine Isotope Stage 3 over the north American continent: sedimentological and mineralogical evidence from the Gulf of Mexico. *Quat. Sci. Rev.* 81, 62–73.
- Skinner, R.G., 1973. Quaternary stratigraphy of the Moose River Basin, Ontario. *Geol. Survey Can. Bull.* 225, 1–77.
- Sosdian, S., Rosenthal, Y., 2009. Deep-Sea Temperature and Ice volume changes across the Pliocene-Pleistocene climate Transitions. *Science* 325 (5938), 306–310.
- Spratt, R.M., Lisiecki, L.E., 2016. A Late Pleistocene sea level stack. *Clim. Past* 12 (4), 1079–1092.
- Stokes, C.R., Tarasov, L., Dyke, A.S., 2012. Dynamics of the North American Ice Sheet complex during its inception and build-up to the Last Glacial Maximum. *Quat. Sci. Rev.* 50, 86–104.
- Stuiver, M., Reimer, P.J., 1993. Extended ^{14}C data base and revised Calib 3.0 ^{14}C age calibration program. *Radiocarbon* 35 (1), 215–230.
- Stuiver, M., Reimer, P.J., Reimer, R.W., 2021. CALIB 8.2 [WWW program] at <http://calib.org>, accessed 2021-12-15.
- Svendsen, J.L., et al., 2004. Late Quaternary ice sheet history of northern Eurasia. *Quat. Sci. Rev.* 23 (11–13), 1229–1271.
- Taylor, R.E., 1987. Chapter 5 - Evaluation of radiocarbon data. In: Taylor, R.E. (Ed.), *Radiocarbon Dating an Archaeological Perspective*. Academic Press, pp. 105–146.
- Thorleifson, L.H., Wyatt, P.H., Shilts, W.W., 1992. Hudson Bay lowlands Quaternary stratigraphy: evidence for early Wisconsinan glaciation centred in Quebec. *Geol. Soc. Am. Spec. Pap.* 270, 207–221.
- Tierney, J.E., et al., 2020. Glacial cooling and climate sensitivity revisited. *Nature* 584, 569–573.
- Tripanas, E.K., et al., 2007. Sedimentological history of Bryant Canyon area, Northwest Gulf of Mexico, during the last 135 kyr (Marine Isotope Stages 1–6): a proxy record of Mississippi River discharge. *Palaeogeogr. Palaeoclimatol. Palaeoecol.* 246 (1), 137–161.
- Tyrrell, J.B., 1898. The glaciation of north Central Canada. *J. Geol.* 6 (2), 147–160.
- Ukkonen, P., Lunkka, J.P., Jungner, H., Donner, J., 1999. New radiocarbon dates from Finnish mammoths indicating large ice-free areas in Fennoscandia during the Middle Weichselian. *J. Quat. Sci.* 14 (7), 711–714.
- Ukkonen, P., Arppe, L., Houmark-Nielsen, M., Kjær, K.H., Karhu, J.A., 2007. MIS 3 mammoth remains from Sweden—implications for faunal history, palaeoclimate and glaciation chronology. *Quat. Sci. Rev.* 26 (25), 3081–3098.
- Ullman, D.J., et al., 2015. Southern Laurentide ice-sheet retreat synchronous with rising boreal summer insolation. *Geology* 43 (1), 23–26.
- Väilänta, M., Sarala, P., Eskola, T., 2012. Uusia todisteita boreaalista olosuhteista Veiksel-interstadiaalin aikana. [with English summary]. *Geologi* 64, 9–14.
- Waelbroeck, C., et al., 2002. Sea-level and deep water temperature changes derived from benthic foraminifera isotopic records. *Quat. Sci. Rev.* 21 (1), 295–305.
- Walczak, M.H., et al., 2020. Phasing of millennial-scale climate variability in the Pacific and Atlantic Oceans. *Science* 370 (6517), 716.

- Ward, B.C., Bond, J.D., Gosse, J.C., 2017. Evidence for a 55–50 ka (early Wisconsin) glaciation of the Cordilleran ice sheet, Yukon Territory, Canada. *Quat. Res.* 68 (01), 141–150.
- Wohlfarth, B., 2010. Ice-free conditions in Sweden during Marine Oxygen Isotope Stage 3? *Boreas* 39 (2), 377–398.
- Woillard, G.M., Mook, W.G., 1982. Carbon-14 Dates at Grande Pile: Correlation of land and sea chronologies. *Science* 215, 159–161.
- Wood, J.R., Forman, S.L., Everton, D., Pierson, J., Gomez, J., 2010. Lacustrine sediments in Porter Cave, Central Indiana, USA and possible relation to Laurentide ice sheet marginal positions in the middle and late Wisconsinan. *Palaeogeogr. Palaeoclimatol. Palaeoecol.* 298 (3–4), 421–431.
- Yokoyama, Y., Esat, T.M., Lambeck, K., 2001. Coupled climate and sea-level changes deduced from Huon Peninsula coral terraces of the last ice age. *Earth Planet. Sci. Lett.* 193 (3), 579–587.
- Young, J.M., Reyes, A.V., Froese, D.G., 2021. Assessing the ages of the Moorhead and Emerson phases of glacial Lake Agassiz and their temporal connection to the Younger Dryas cold reversal. *Quat. Sci. Rev.* 251, 106714.
- Zachos, J., Pagani, M., Sloan, L., Thomas, E., Billups, K., 2001. Trends, rhythms, and aberrations in global climate 65 Ma to present. *Science* 292 (5517), 686–693.
- Zhang, X., Lohmann, G., Knorr, G., Purcell, C., 2014. Abrupt glacial climate shifts controlled by ice sheet changes. *Nature* 512, 290–294.